

12-2008

# THE EFFECT OF MONTMORILLONITE NANOCLAY ON MECHANICAL AND BARRIER PROPERTIES OF MUNG BEAN STARCH FILMS

Bianca Stiller

Clemson University, [bstille@clemson.edu](mailto:bstille@clemson.edu)

Follow this and additional works at: [https://tigerprints.clemson.edu/all\\_theses](https://tigerprints.clemson.edu/all_theses)

 Part of the [Engineering Commons](#)

---

## Recommended Citation

Stiller, Bianca, "THE EFFECT OF MONTMORILLONITE NANOCLAY ON MECHANICAL AND BARRIER PROPERTIES OF MUNG BEAN STARCH FILMS" (2008). *All Theses*. 504.

[https://tigerprints.clemson.edu/all\\_theses/504](https://tigerprints.clemson.edu/all_theses/504)

This Thesis is brought to you for free and open access by the Theses at TigerPrints. It has been accepted for inclusion in All Theses by an authorized administrator of TigerPrints. For more information, please contact [kokeefe@clemson.edu](mailto:kokeefe@clemson.edu).

THE EFFECT OF MONTMORILLONITE NANOCCLAY ON MECHANICAL AND  
BARRIER PROPERTIES OF MUNG BEAN STARCH FILMS

---

A Thesis  
Presented to  
the Graduate School of  
Clemson University

---

In Partial Fulfillment  
of the Requirements for the Degree  
Master of Science  
Packaging Science

---

by  
Bianca Stiller  
December 2008

---

Accepted by:  
Dr. Scott Whiteside, Committee Chair  
Dr. Ron Thomas  
Dr. Kay Cooksey

## ABSTRACT

Starch is an interesting biodegradable polymer due to its excellent film forming properties, availability, and low cost. On the other hand, starch films are often limited by their poor mechanical properties, and water resistance. The addition of montmorillonite clays have improved these properties in both petroleum and biodegradable films. The objective of the research was to determine the effect of montmorillonite clay on the mechanical and barrier properties on mung bean starch films. The addition of 5% clay yielded the optimum balance between mechanical and barrier properties of these composite films with improved tensile strength (TS) of  $20.8763 \pm 0.789$  MPa, decreased water vapor permeability (WVP) to  $0.49150 \pm 0.0502$  ng m/m<sup>2</sup> sPa and decreased oxygen permeability (OP) to  $5.84 \pm 1.10$  cc-mil/(m<sup>2</sup>-day). Clay levels above 5% improved water vapor barrier properties, with greatest results for 25 and 30% clay of  $0.4519 \pm 0.0603$  and  $0.4405 \pm 0.0826$ , respectively. However, the films became brittle with the further addition of clay and had lower TS values and % elongation at break (EB) values. X-Ray Diffraction showed exfoliated clay microstructures for films with lower clay amount. Above 10% clay, intercalated montmorillonite clay layers and clay were obtained. TEM images confirmed the X-Ray results. The highest ultrasonication times of 30 and 60 minutes (5%wt clay) yielded the highest TS values,  $20.6083 \pm 1.330$  and  $20.4281 \pm 1.355$  MPa, respectively. Ultrasonication time had no effect on EB. Oxygen permeability decreased as ultrasonication time increased to minimum permeability of  $2.36 \pm 0.27$  cc-mil/(m<sup>2</sup>-day).

WVP decreased as ultrasonification time increased with the lowest value at 5 minutes ultrasonification of  $0.5269 \pm 0.0712$  ng m/m<sup>2</sup> sPa. The X-Ray results as well as the TEM images determined exfoliated structures for higher ultrasonification times of 30 and 60 minutes and intercalated structures for lower ultrasonification times.

## DEDICATION

I dedicate this work to my fiancé Andrew Hurley, whose love and support have deeply inspired and encouraged me.

## ACKNOWLEDGMENTS

I would like to express my appreciation to my advisor, Dr. Scott Whiteside, for his guidance in this research, his academic advises and knowledge. I would like to thank the members of my committee, Dr. Kay Cooksey and Dr. Ron Thomas, for their advice, insights and review of my thesis. I would also like to thank Dr. Darby for great assistance with ASTM standards. A sincere thank goes to my office member Dr. Bae for consistently helping and inspiring me with my research as well as Young Jae Byun for your knowledge and brainstorming. I would like to thank Dr. Ingo Sabotka for supporting me with the exchange opportunity before and during this program. I also would like to thank Dr. Kimmel and Dr. Batt for making it possible for me to study abroad at Clemson University. Thank you to Mr. Bob Moore who always put a smile on my face. Thank you to Mr. Rijosh J. Cheruvathur for introducing me to the challenging world of permeability. I want to thank Sunil Mangalassary and Chike Ifezue for being great lab and office neighbors, for talks and advices. I would like to thank Mrs. Alison Tusso for feeding me with German treats. I also want to thank Dr. Young T. Kim for fast help on a Sunday morning. Special thanks to my fiancé, Andrew Hurley, for great mental support, patience and calming influence and being there for me. Special thank to my family for always supporting me. Thank you to Christian for friendship and assistance with chemical questions and formation issues. Thank you to the members of the German “BSE-Team”, Steffen and Ebuel. I also would like to thank my friends, specially Sabrina, Jenny, Nadine, Stephan, Christiane, Axel and Conny.

## TABLE OF CONTENTS

|  | Page |
|--|------|
| TITLE PAGE .....                               | i    |
| ABSTRACT .....                                 | ii   |
| DEDICATION .....                               | iv   |
| ACKNOWLEDGMENTS .....                          | v    |
| TABLE OF CONTENTS .....                        | vi   |
| LIST OF TABLES .....                           | viii |
| LIST OF FIGURES .....                          | x    |
| I. INTRODUCTION .....                          | 1    |
| <b>Problem Definition</b> .....                | 1    |
| <b>Objectives</b> .....                        | 3    |
| II. LITERATURE REVIEW .....                    | 4    |
| <b>Biodegradable Packaging</b> .....           | 4    |
| <b>Overview of biopolymers</b> .....           | 6    |
| <b>Starch</b> .....                            | 7    |
| Starch Properties .....                        | 10   |
| Common Starch Films .....                      | 11   |
| Mung Bean Starch .....                         | 13   |
| <b>Montmorillonte Clay</b> .....               | 14   |
| <b>Theoretical Materials and Methods</b> ..... | 19   |
| Preparation Solution .....                     | 19   |
| Connection Clay and Starch .....               | 20   |
| Film Formation .....                           | 23   |
| <b>Properties</b> .....                        | 24   |
| Mechanical Properties .....                    | 24   |
| Barrier Properties .....                       | 25   |

**Table of Contents (Continued)**

|   |    |
|---|----|
| Optical characterization .....                      | 33 |
| Microstructural Analysis.....                       | 34 |
| III EXPERIMENTAL DESIGN .....                       | 39 |
| <b>Materials</b> .....                              | 39 |
| <b>Methods</b> .....                                | 39 |
| <b>Composition Batches</b> .....                    | 41 |
| IV. RESULTS AND DISCUSSION.....                     | 48 |
| <b>X-Ray Diffraction\</b> .....                     | 48 |
| <b>Transmission Electron Microscopy (TEM)</b> ..... | 51 |
| <b>Tensile Strength</b> .....                       | 56 |
| <b>% Elongation at Break</b> .....                  | 59 |
| <b>Oxygen Permeability</b> .....                    | 61 |
| <b>Water Vapor Permeability</b> .....               | 63 |
| <b>Color and Haze</b> .....                         | 66 |
| V. CONCLUSIONS.....                                 | 70 |
| VI. FUTURE RESEARCH.....                            | 72 |
| REFERENCES .....                                    | 74 |



## LIST OF TABLES

| Table | Page   |
|-------|--|
| 1     | Classification of Biopolymers..... 6                                   |
| 2     | Comparison of Thermoplastic Starch, Destructive Starch and TPS..... 11 |
| 3     | Classification Clay ..... 14   |
| 4     | Swelling of Montmorillonite..... 17                                    |
| 5     | Connection methods of clay and starch ..... 20                         |
| 6     | Definition WVT and WVP. .... 30  |
| 7     | Water Vapor Transmission calculation..... 31                           |
| 8     | Water Vapor Permeance calculation..... 31                              |
| 9     | Calculation Haze..... 33   |
| 10    | Calculation of Color Difference..... 34                                |
| 11    | Variable Braggs Law ..... 35   |
| 12    | Ultrasonification Batch Identification..... 42                         |
| 13    | Clay Batch Identification ..... 43                                     |
| 14    | Composition Batch S60C10..... 44                                       |
| 15    | Oxygen Permeability, batch ultrasonification time ..... 61             |
| 16    | Oxygen Permeability, batch amount clay ..... 62                        |
| 17    | Water Vapor Permeability, batch ultrasonification time ..... 64        |
| 18    | Water Vapor Permeability: Batch Amount Clay ..... 65                   |
| 19    | Color measurements: Batch ultrasonification time..... 66               |

**List of Tables (Continued)**

| Table   | Page |
|---|------|
| 20 Color measurements, Batch amount clay..... | 68   |
| 21 Appearance composite films.....            | 69   |

## LIST OF FIGURES

| Figure  | Page |
|---|------|
| 1 Molecular Structure of Starch.....                          | 8    |
| 2 Structure of Montmorillonite.....                           | 15   |
| 3 Increased layer space due to swelling of Clay.....          | 18   |
| 4 Tortuous Path.....  | 19   |
| 5 Ionic attraction between Na <sup>+</sup> ion and Water..... | 21   |
| 6 Interaction of Na <sup>+</sup> ion and hydroxyl group.....  | 21   |
| 7 Different clay dispersion in polymer matrix.....            | 22   |
| 8 Ultrasonification Technique.....                            | 23   |
| 9 Stress-Strain curve.....                                    | 25   |
| 10 The material transport trough a polymer film.....          | 27   |
| 11 Oxygen Transmission Rate Testing Apparatus.....            | 29   |
| 12 Stagnant air layer in test dish for WVP (ASTM E96).....    | 32   |
| 13 Explanation Bragg's Law.....                               | 35   |
| 14 Method of operation of TEM.....                            | 38   |
| 15 Film cracking due to low casting speed.....                | 41   |
| 16 X-Ray Pattern, Batch Ultrasonification Time.....           | 48   |
| 17 X-Ray Pattern, Batch Clay Amount.....                      | 50   |
| 18 TEM images, Batch Ultrasonicatin Time.....                 | 53   |
| 19 TEM images, Batch Clay Amount.....                         | 55   |

**List of Figures (Continued)**

| Figure   | Page |
|--|------|
| 20 Tensile Strength Results, Batch Ultrasonification Time..... | 56   |
| 21 Tensile Results, Batch Clay Amount .....                    | 58   |
| 22 % Elongation at Break, Batch Ultrasonification Time .....   | 59   |
| 23 % Elongation at Break, Batch Clay Amount .....              | 60   |

# CHAPTER ONE

## I. INTRODUCTION

### **Problem Definition**

"The [current] pattern of resource use will lead to a collapse of the world system within the next century. These were the words of that hit the headlines when the world was shaken by the oil crisis in 1973." (Hamerton, 2003).

Since 1973, biopolymer materials have been the subject of much research and investigation. There are several biopolymer materials that have been used in commercial applications. Cellophane, invented by Jacques E. Brandenberger, is the oldest biodegradable, transparent packaging material. It has average water vapor permeability, excellent machinability, and heat sealability. Due to increasing environmental concerns, this cellulose based material is regaining popularity (Bellis, 1997). Another biodegradable polymer that has also a long history of use is gelatin. Gelatin has traditionally been utilized as thickener for many food products and sausage casings and it is commonly used to form both hard and soft biodegradable capsules for the pharmaceutical industry (Stevens, 2002). Polylactic acid (PLA) has recently become a very important material based on its thermoplastic properties and ability to offer reasonable shelf life for various packaging applications. Natureworks is one of the main supplier of PLA products (Steinbuechel, 2003 and Stevens, 2002). Procter & Gamble (P & G, USA) has developed biodegradable PHA polymers for use in films, fibers and

molded components. Thermoplastic starch polymers have been developed by Novamont, and similar companies, to produce such products as mulch films, bags and thermoformed packages (Smith, 2000). Biodegradable packaging has the advantage, unlike petroleum based polymer, to break down more rapidly by enzymes into natural substances (i.e. minerals, salts, water and CO<sub>2</sub>). The demand for such environmentally friendly polymers is growing and has been focus of many researcher efforts (Darder et.al., 2007).

Sustainable and biodegradable packages are being developed worldwide. Unfortunately, biodegradable packages are either associated with high manufacturing costs or their performance is inadequate for many applications. In an effort to bring more biodegradable polymers into the marketplace, research is focused on enhancing the properties of biodegradable polymers. Starch based polymers are highly water soluble and have low mechanical strength, yet show excellent oxygen barrier (Bertuzzi et al., 2006). Thus, it is useful to connect starch-based polymers with another biodegradable additives to improve performance properties. Former research on starch composites have improved properties (barrier and mechanical) by using only small quantities filler concentrations of nanoclay (Cyras et al., 2007., Chaudhary, 2008). Research also illustrates that starches with higher amylase content form more desirable biodegradable materials with greater mechanical improvements than high amylopectin starches (Bae et al., 2007, Mondragon et al., 2008). The concept of combining clay with a high amylase starch has the potential of improving the attributes of starch-based polymers.

## **Objectives**

The field of biodegradable plastics has been well researched. Yet there are few satisfactory alternatives for many conventional polymers. Development of material properties with both process and cost feasibility have been an ongoing challenge for polymer scientists (Smith, 2000). Starch has been shown to be an inexpensive and readily available alternative to oil derived polymers, however, it has poor mechanical properties and limited water permeability. A composite of starch and another additive might be a solution to improve these properties. The application of nanotechnology has great potential for adding value to materials for the packaging industry. Nanoclay is one example of an additive that is widely available, cost effective, biodegradable and has been shown to improve the properties of various polymer materials. To adequately understand the effect on physical and mechanical properties of starch nanocomposite films, much work is required. Mung bean starch has proven to be excellent material for biodegradable films with good oxygen barrier properties. However, its limited water vapor permeability and mechanical strength could be improved by adding nanoclay to the mung bean starch matrix.

Therefore, this research focused on characterizing the effects of montmorillonite nanoclay on the mechanical and barrier properties of mung bean starch films.

## CHAPTER TWO

### II. LITERATURE REVIEW

#### **Biodegradable Packaging**

When discussing biodegradable packaging, it is important to differentiate between biodegradable, degradable, compostable, and sustainable plastics. A biodegradable plastic is defined as a plastic in which the degradation results from the action of naturally occurring microorganisms such as bacteria, fungi and algae. A degradable plastic is a plastic designed to undergo a significant change in its chemical structure under specific environmental conditions resulting in loss of properties. A compostable plastic is defined as a plastic that undergoes degradation by biological processes during composting to yield CO<sub>2</sub>, water, inorganic compounds, and biomass at a rate consistent with other compostable materials and leaves no visible, distinguishable or toxic residue (ASTM D 883). The Sustainable Packaging Coalition defines sustainable packaging as satisfying the following criteria:

- A. Is beneficial, safe & healthy for individuals and communities throughout its life cycle
- B. Meets market criteria for performance and cost
- C. Is sourced, manufactured, transported, and recycled using renewable energy
- D. Maximizes the use of renewable or recycled source materials



- E. Is manufactured using clean production technologies and best practices
- F. Is made from materials healthy in all probable end of life scenarios;
- G. Is physically designed to optimize materials and energy
- H. Is effectively recovered and utilized in biological and/or industrial cradle to cradle cycles.

(The Sustainable Packaging Coalition, 2005)

Biodegradable polymers are considered environmentally safe based on their ability to decompose into minor naturally occurring compounds thereby providing a sustainable alternative to traditional petroleum based plastics. Sustainable polymers are capable of existing with minimal long-term effect on the environment (Hamerton, 2003). Sustainable biodegradable polymers, such as thermoplastic starch are also readily available due to their mass production for use in the food industry. Oil based plastics require a relatively long time to degrade into their natural elements thereby creating various environmental concerns. The worldwide acceptance and production of biodegradable products is increasing dramatically. "The current worldwide consumption of biodegradable polymers has increased nearly eight times from the production of 14 million kg in 1996 (Smith, 2000)." However, increased production of many of these sustainable biopolymers can result or create other concerns. The increased demand for the base raw materials can often have a negative impact on the price and supply of many competing products. For example, the increasing amount for corn used for the

production of PLA can increase the price and decrease the supply of corn available for animal and human feed or ethanol production. Also, an integrated waste management system is necessary in order to efficiently use, recycle and dispose of the biodegradable materials. (Subramanian, 2000).

### Overview of biopolymers

Biopolymers can be classified into two main groups, biopolymers from natural origins and biopolymers from mineral origins.

**Table 1: Classification of Biopolymers**

|          | <b>Biopolymers from nature origins</b>   | <b>Biopolymers from mineral origins</b>  |
|----------|--|--|
| <b>1</b> | Polysaccharide (e.g., starch, cellulose, lignin, chitin)   | Aliphatic polyester (e.g., polyglycolic acid, polybutylene succinate, polycaprolactone)                    |
| <b>2</b> | Proteins (e.g., gelatin, casein, wheat gluten, silk and wool)  | Aromatic polyesters or blends of the two types (e.g., polybutylene succinate terephthalate)                |
| <b>3</b> | Lipids (e.g., plant oils including castor oil and animal fats)   | Polyvinylalcohols  |
| <b>4</b> | Polyester produced by micro-organism or by plants (e.g., polyhydroxy-alcanoates, poly-3-hydroxybutyrate) | Modified polyolefin (polyethylene or polypropylene with specific agents sensitive to temperature or light) |
| <b>5</b> | Polyester synthesized from bio-derived monomers (polylactic acid)  | -  |
| <b>6</b> | Miscellaneous polymers (nature rubbers, composites)  | -  |

Source: Smith, 2000

The use of biodegradable polymers from natural polysaccharides is popular based on a long history of use, availability and relatively low costs compared to other biopolymers. Therefore starch, as a natural polysaccharide, has the potential to be a viable alternative to many traditional oil based plastics.

## **Starch**

Starch is a commonly used food product. Starch bioplastics are made from thermoplastic starch and formed with standard techniques for synthetic polymer films such as extrusion or injection moulding (Mallapragada et al., 2006). Starch (Figure 1) is a polysaccharide consisting of long, helical chains of amylose and amylopectin. Starch can be produced from plants like corn, wheat, potato, cassava and beans. Because starch can be easily gelatinized, it is useful for the production of biodegradable films. Gelatinization refers to the disruption of molecular order within starch granules as they are heated in the presence of water (Whistler, 1997). Starch is an energy reserve for many plants and is mainly composed of carbohydrates (glucose, a six-carbon aldehyde with five hydroxyl groups (Mc Murry, 2001)) Starch is a physical combination of linear and branched polymers, the amylose (normally 20-30%) and amylopectin (normally 70-80%). While the amylose is nearly linear, the amylopectin is highly branched and consists of side chains. Both consist of  $\alpha$ -(1-4) glucosidic bonds (1-4 are the bonding positions). Amylopectin also has a bond at the branch point at  $\alpha$ -(1-6).

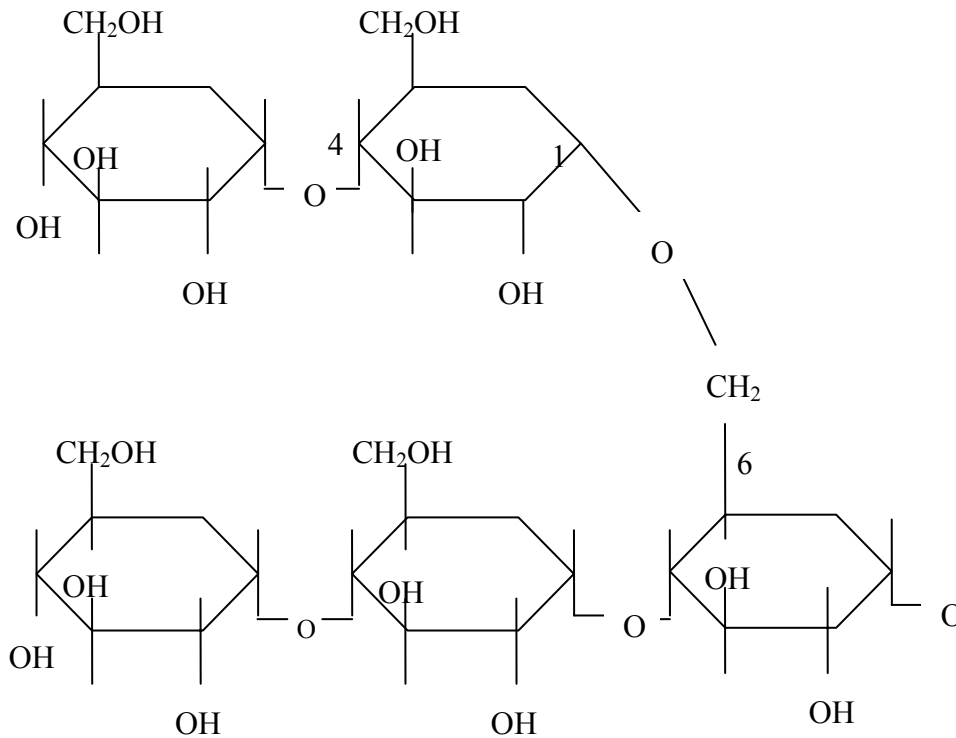


**Figure 1: Molecular Structure of Starch**

Source: Redrawn from Whistler, 1984.

Amylose chains are spiraled or helical in shape, which gives films a high elasticity (Whistler, 1994).

Natural starches form granules (discrete particles, in amyloplast of plant, which can be dispersed in water, producing low viscosity slurries, containing a mixture of 2 polymers) where the amylose and amylopectin are structured with hydrogen bonding (Whistler, 1994). A hydrogen bond is an attractive interaction between a hydrogen atom bonded to a very electronegative atom (Mc Murray et al., 2001). Starch molecules are polar

polymers with many OH functional groups which can be hydrogen bonded in water solutions. Polarity refers to an unequal sharing of electrons of molecules (Walter, 1999). Another functional group in the starch polymer is the C-O-C bond which is susceptible to chain breakage. As the amount of amylopectin in the molecule increases, the starch shows a higher crystallinity. “Highly ordered molecular arrangements are said to be crystalline, while completely random arrangements are amorphous” (Mc Murry, 2001). Starch can offer one of three different crystalline patterns: A, B and C. Pattern A is illustrated in wheat and corn. Pattern B is shown in potato and roots. Both have double helices and are both anti parallel but, B types have open channels filled with H<sub>2</sub>O. B patterns are less denser than the A type. Pattern C is a mixture of A and B type and is found in low amylose pea starches (Whistler, 1984).

The starch film properties vary with the plant source from which it is isolated. Different varieties generally have various granule structures and a separate degree of branching of amylose and amylopectin. Starch granules are used for the production of films. One common method of producing starch film is by casting from an aqueous solution. This casting process requires gelatinized starch. Water acts as a plasticizer for the molecules and weakens the intermolecular forces (Whistler, 1984). Plasticizer are mixed into polymers to increase the plasticity. They lower viscosities at lower temperatures (Osswald et al., 1995).

### ***Starch Properties***

Starch is not only one of the most abundant and lowest priced product worldwide, it also has excellent film making properties due to its linear structure. Pure starch is brittle and not usable as a film. Starch must be plasticized for ease of processing (Whistler, 1984 and Smith 2000) . To obtain a starch polymer, one must choose between destructive or thermoplastic developments. Both are obtained under heat and mechanical forces which result in destruction of the crystalline linkages in the starch granules. After destruction, amorphous regions appear in the polymer structure. The difference between destructive starch and thermoplastic starch is that the thermoplastic starch includes nonvolatile plasticizers (e.g., glycerol/polyols) (Smith, 2000). Thus, destructive starch is not considered a true thermoplastic polymer, but it is often considered thermoplastic because it is processed similarly. Table 2 summarizes the definitions of destructive, thermoplastic and TPS:

**Table 2: Comparison of Thermoplastic Starch, Destructive Starch and TPS**

| <b>Thermoplastic Starch</b>  | <b>Destructive starch</b>   | <b>Thermoplastically Processable Starch (TPS)</b>  |
|--|---|--|
| <ul style="list-style-type: none"> <li>• Gelatinized by extrusion cooking technology</li> <li>• Processed as a traditional plastic</li> <li>• Can be made thermoplastic with low water contents (&lt;10%)</li> </ul> | <ul style="list-style-type: none"> <li>• Form of thermoplastic starch</li> <li>• Molecularly dispersed in water</li> <li>• Suitable for plastic applications</li> </ul> | <ul style="list-style-type: none"> <li>• Is substantially water free</li> <li>• Modified native starch</li> <li>• Made of a plasticizer or additive</li> </ul> |

Source: Steinbuechel (2003).

Once a destructive or thermoplastic starch is produced, the polymer is usually translucent and provides a low permeability to oxygen, has an antistatic behavior, is soft and silky to handle, has colorability and is compostable (Steinbuechel, 2003). These films also show high permeability to water and water vapor but can be degraded by amylases and or glycosidase.

***Common Starch Films***

Due to their excellent film forming properties, availability and low costs, different starches have been widely used for the production of starch based films. Research has

focused on improving the water vapor permeability and mechanical properties of starch based films.

Commercial cassava starch films have been developed to determine physiochemical properties. Results indicated that starch concentration and type can be related to permeability, solubility and thickness of produced films (Henrique C.M. et al., 2007). Corn starch edible films with excellent transparency were produced by Bertuzzi et al. Their research demonstrated the influence of factors such as plasticizer content and film thickness and their effect on the water vapor permeability of corn starch films (Bertuzzi et al., 2006).

High amylose rice starch and pea starch films have been produced in an effort to determine their mechanical and barrier properties. The study indicated that the ease of preparation along superior mechanical and barrier properties of these starches increase their potential applications for food preservation (Mehyar et al., 2004).

Potato, sweet potato, waterchestnut and mung bean starch films have also been produced to determine formation properties compared to gelatin based films. Results indicated that these starch films had good mechanical and physical properties when compared to gelatin films. Waterchestnut and mung bean starch produced better films than potato and sweet potato starches, due to their high amylose content. Mung bean starch showed the highest tensile strength values when compared with all starch films (Bae et al., 2007).



### ***Mung Bean Starch***

Mung bean belongs to genus *Vigna* and species *Radiata*. Mung beans need a warm, tropical environment for best cultivation. Mung beans consist of small beans which are green or in some cases also brown in skin color. Under the skin, they have a yellow color. Mung beans are also known under the names such as green beans, mung, moong and green grams. The leading production country of mung bean is India, where the bean is also native. The seeds are also widely used in China, Korea and Southeast Asia. The major use of mung beans is for the food industry. Mung beans can be eaten whole or as bean sprouts and they can be used for producing deserts such as ice cream. The starch from mung beans can be separated from ground mung beans. Due to an high amylase (30%) content in mung bean starch, it easily forms gels. Another common application for mung bean starch is the production of “cellophane” noodles. These noodles have a transparent appearance and are also referred to as “glass noodles” (Brown, 1991 and IT IS report, 2008). In addition to these food applications, mung bean starch can also be used for the production of transparent starch based films. In fact, the amylose content of starch is an important factor for producing a biodegradable film. Starches with higher amylase content (>20%) form better biodegradable films than starches containing less amylase (Bae et al, 2007 and Lawton, 1996). Prior research indicated that mung bean starch, with a high amylase content (30%), produces proper films, with improved film forming, mechanical and barrier properties compared to low amylase starches (Bae et al., 2007). Therefore mung bean starch was selected as the base material for this research.

## Montmorillonite Clay

Clays encompass a diverse group of naturally granulated clay minerals and can be divided into two main groups (see Table 3).

"Clays are hydrous silicates or aluminum silicates and may broadly be defined as those minerals which dominantly make up the colloidal fraction of soils, sediments, rocks, and waters" (Theng, 1979).

**Table 3: Classification Clay**

| <b>Aluminum Silicates</b>   | <b>Individual Clay minerals</b>   |
|---|---|
| <ul style="list-style-type: none"><li>• Contains water and cations (e.g. iron, sodium, lithium, magnesium)</li><li>• Sheeted atomic structure</li></ul> | <ul style="list-style-type: none"><li>• Mixtures of clay minerals and other mineral components</li><li>• often silica, cristobalite or mica</li></ul> |

Montmorillonite is the main component of bentonite. Bentonite is a volcanic rock deposited as ash in water. Montmorillonite clay is composed of a tetrahedral sheet of  $\text{SiO}_4$ , an octahedral coordinated sheet of aluminum, magnesium or iron, sandwiched between another tetrahedral sheet of  $\text{SiO}_4$  (Clarke, 1989). Montmorillonite is typically a sodium rich rock.

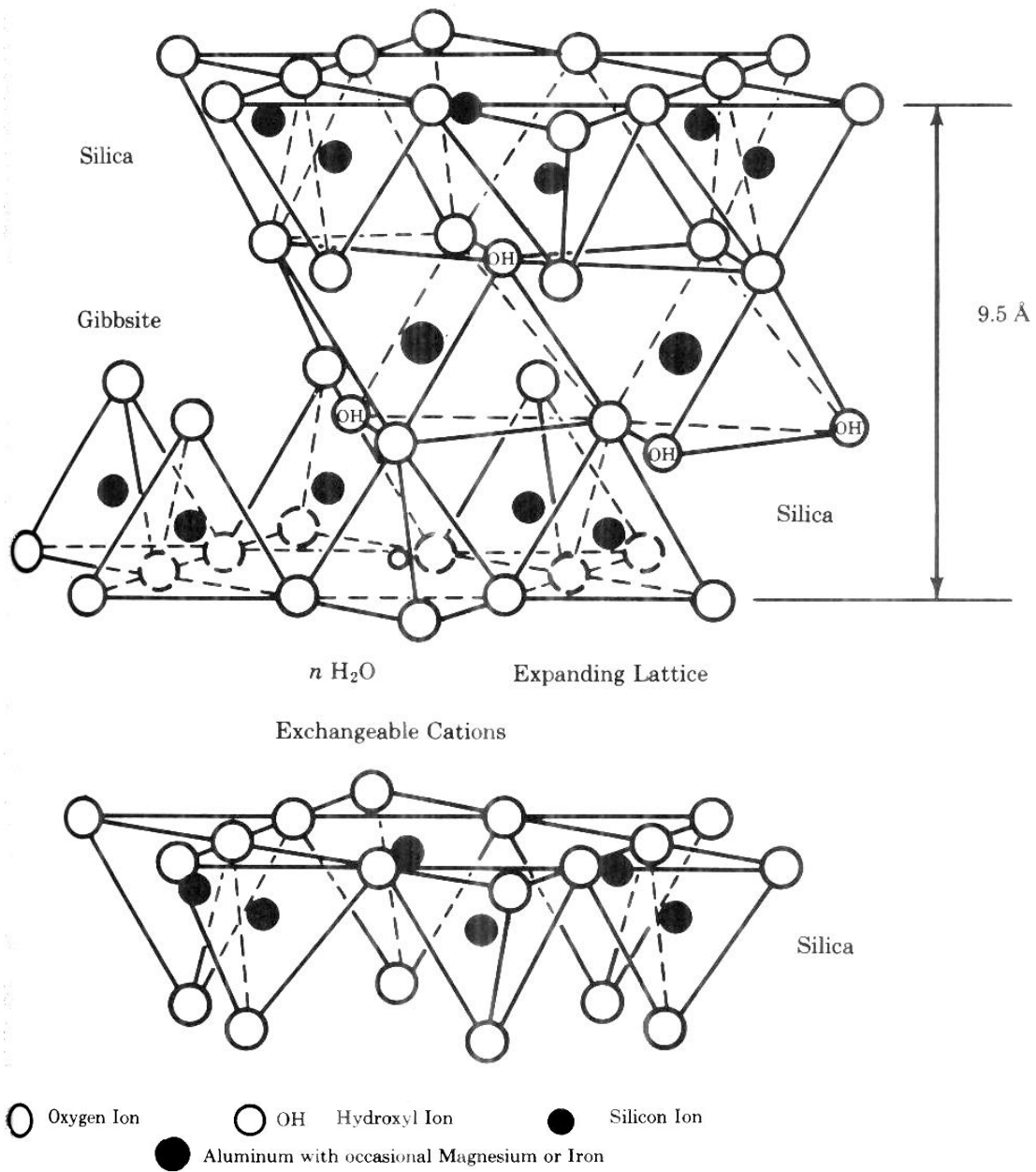


**Figure 2: Structure of Montmorillonite**

Source: Means, 1963.

Montmorillonite resembles a crystal around 2 microns in size. The form is plate like, very thin, and has a large surface area (  $800\text{m}^2/\text{gm}$ ). Due to the inside layer, a negative charge imbalance is created at the layer surface along with the probability of cation exchange. In montmorillonite,  $\text{Na}^+$  ions can be exchanged in water with any other metal.

Montmorillonite also has a high swelling capacity due to hydration of the interlayer sodium (see Figure 2). The hydration of cations present in montmorillonite imparts a hydrophilic nature of the clay surface (Memut, 1994). The sodium cation can take up water which creates an interlayer spacing. Swelling of sodium montmorillonite can be described in 3 states:

**Table 4: Swelling of Montmorillonite**

| <b>Swelling State</b> | <b>Description</b>  |
|-----------------------|---|
| 1)                    | <ul style="list-style-type: none"> <li>• crystalline swelling</li> <li>• due to hydration of interlayer polyvalent cation (Polyvalent cation is a species of cations that are not singularly valent. This means that the species of cations can contain multiple valencies, i.e. Fe<sup>+</sup> could become Fe<sup>++</sup> or Fe<sup>+++</sup> (Murray, 2001)</li> <li>• separation around 1nm</li> </ul> |
| 2)                    | <ul style="list-style-type: none"> <li>• monovalent cations (na<sup>+</sup>) take up more water</li> <li>• abruptly increase of spacing 3-4 nm</li> <li>• Formation of diffuse electrical double layers on interlayer surfaces</li> <li>• Paste now becomes thick gel</li> </ul>  |
| 3)                    | <ul style="list-style-type: none"> <li>• Separated layers by large distance</li> <li>• Due to shaking</li> </ul>  |

Source: Theng, 1979

Sodium bentonite can swell 8 to 15 times its dry weight. Theoretically, this allows the integration of the nanoclay with the starch matrix. Figure 3 shows the increase of the space between clay-interlayers.

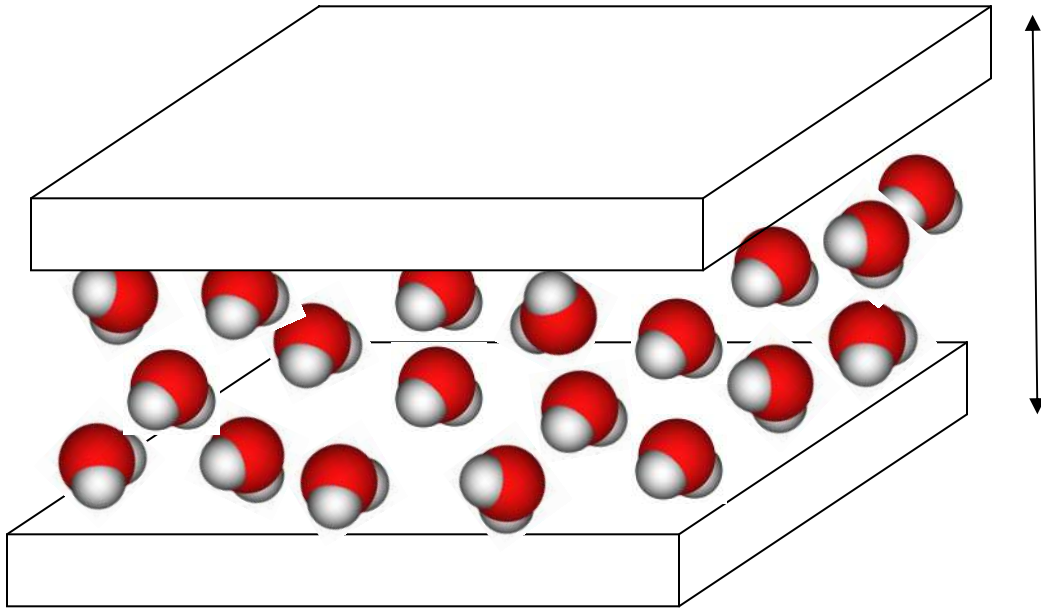


**Figure 3: Increased layer space due to swelling of Clay**

Recent modifications to montmorillonite have improved the bond between clay and conventional plastic matrix. Organophilic (water fearing) clays are examples for those modified nanoclays. Organophilic clays can be formed by exchanging ammonium compounds onto the silicate layers what makes them compatible with conventional polymers (Mermut, 1994).

Unmodified montmorillonite layers are hydrophilic (water loving). For the case of starch, unmodified clays are compatible with hydrophilic starch matrix. The starch is able to

penetrate through the interlayer of the clay, promoting the barrier and increasing film properties. Well dispersed clay particles form a tortuous path, consequently, molecules and gas have to find a way through this path thereby improving barrier properties.

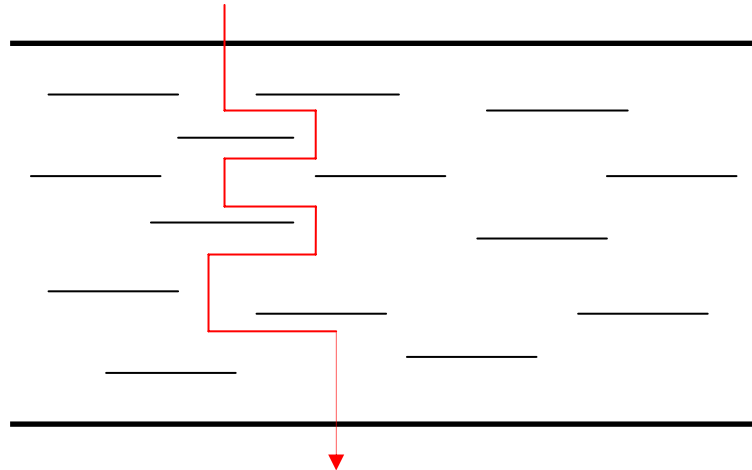


**Figure 4: Tortuous Path**

While modified clays have good compatibility with conventional oil based films, unmodified montmorillonite is useful for the production of starch-clay composite films.

## **Theoretical Materials and Methods**

### ***Preparation Solution***

To obtain a transparent starch solution, starch granules must be completely gelatinized in distilled water at an optimal time-temperature ratio. If the starch-water concentration is too low, the film will not cast properly. If the concentration is too high, the solution becomes too viscous to cast a proper film. The suggested solid concentration is between

10% and 15% starch. The optimum gelatinization temperature based on the specific starch variety used. Starches with lower amylose contents are usually gelatinized at lower temperatures when compared to starches with higher amylose content. The correct temperature is different for each starch. The temperature range for mung bean starch should rise to 95°C to reach final viscosity (Bae et al., 2007). It is critical that starch does not degrade, thus heat should be gradually increased.

***Connection Clay and Starch***

Prior research describes different ways of connecting nanoclay with starch (Table 5).

**Table 5: Connection methods of clay and starch**

| <b>In-situ polymerization</b>  | <b>Solvent<br/>intercalation/exfoliation</b>  | <b>Melt<br/>intercalation/exfoliation</b>   |
|--|---|---|
| <ul style="list-style-type: none"> <li>• combination of clay and monomer</li> <li>• polymerisation of monomer which locks exfoliated clay in matrix</li> </ul> | <ul style="list-style-type: none"> <li>• clay is swollen in a solvent</li> <li>• polymer is dissolved in solvent</li> <li>• combining of solutions</li> </ul> | <ul style="list-style-type: none"> <li>• clay and polymer are added together above melting temperature of polymer</li> <li>• put under shear or other conditions</li> </ul> |

Since Cloisite Na<sup>+</sup> is hydrophilic (similar to starch), the clay can be dissolved easily within a water/starch solution. The main interaction between water molecules and the



silicate layers of montmorillonite clay is an ion-dipole interaction. The Na<sup>+</sup> ions, which are located between the silicate layers (see Figure 2) are attracted to the partial negative ends of the water molecules (Figure 5).

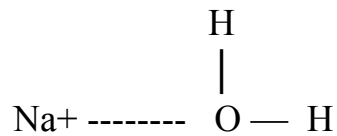


**Figure 5: Ionic attraction between Na<sup>+</sup> ion and Water**

It is also possible that the hydroxyl groups of the montmorillonite layer as well as the hydroxyl groups of the starch interact with the Na<sup>+</sup> ion as illustrated in Figure 6.

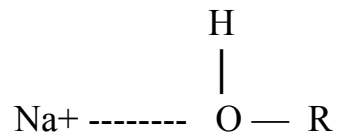


**Figure 6: Interaction of Na<sup>+</sup> ion and hydroxyl group**

Those interactions causes the clay to swell and starch polymers can interact with the layers of montmorillonite.

The two types of desired nanocomposites (intercalated and exfoliated, Figure 6) depend on specific organization of the clay layers. If the polymer is located between increased clay layers, intercalates are obtained. If layer spaces are increased to a point of no attraction, exfoliates are obtained (Krishnamoorti et al., 2002). The level of intercalation

and exfoliation can be measured by X-Ray Diffraction and can be also detected by TEM images.

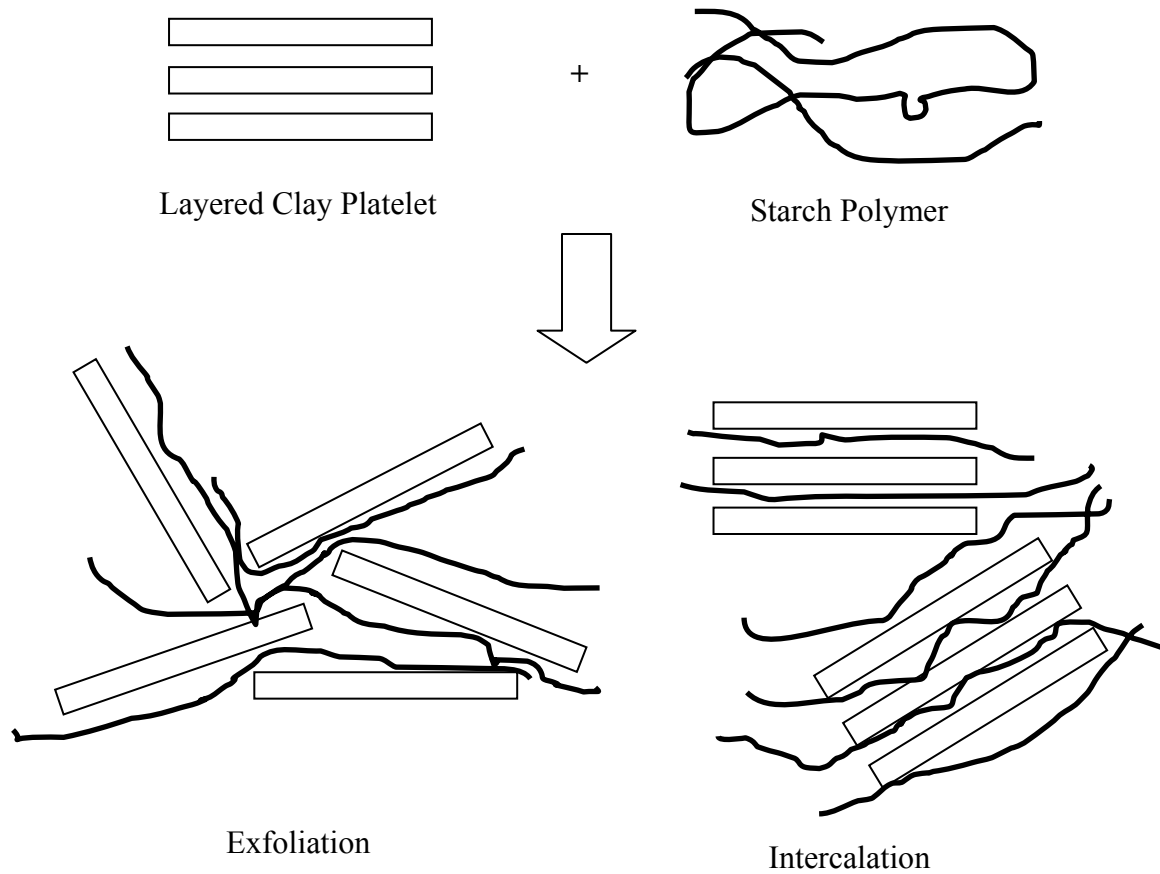


**Figure 7: Different clay dispersion in polymer matrix**

Often, the nanoclay is partially dispersed, resulting in non- exfoliation and partially intercalated platelets . To increase the probability that clay dispersion was optimized, the clay can be ultrasonified before combining with the starch matrix using a sonifier.

Sonifiers utilize with ultrasonic sound waves which cause clay layers to break apart and disperse.

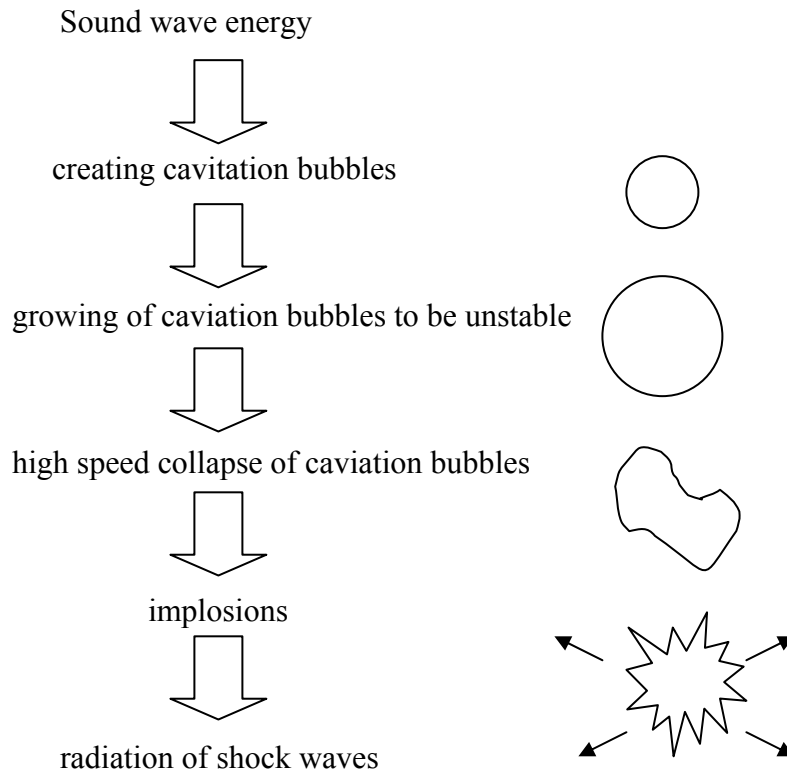


**Figure 8: Ultrasonification Technique**

Source: Smith, 2000.

### ***Film Formation***

Since heated starch tends to retrograde (“the return to an insoluble state” (Whistler, 1997) while cooling, the film should be casted immediately after gelatinizing. To produce a useful film, the prepared solution is casted on a smooth surface. The film has to dry

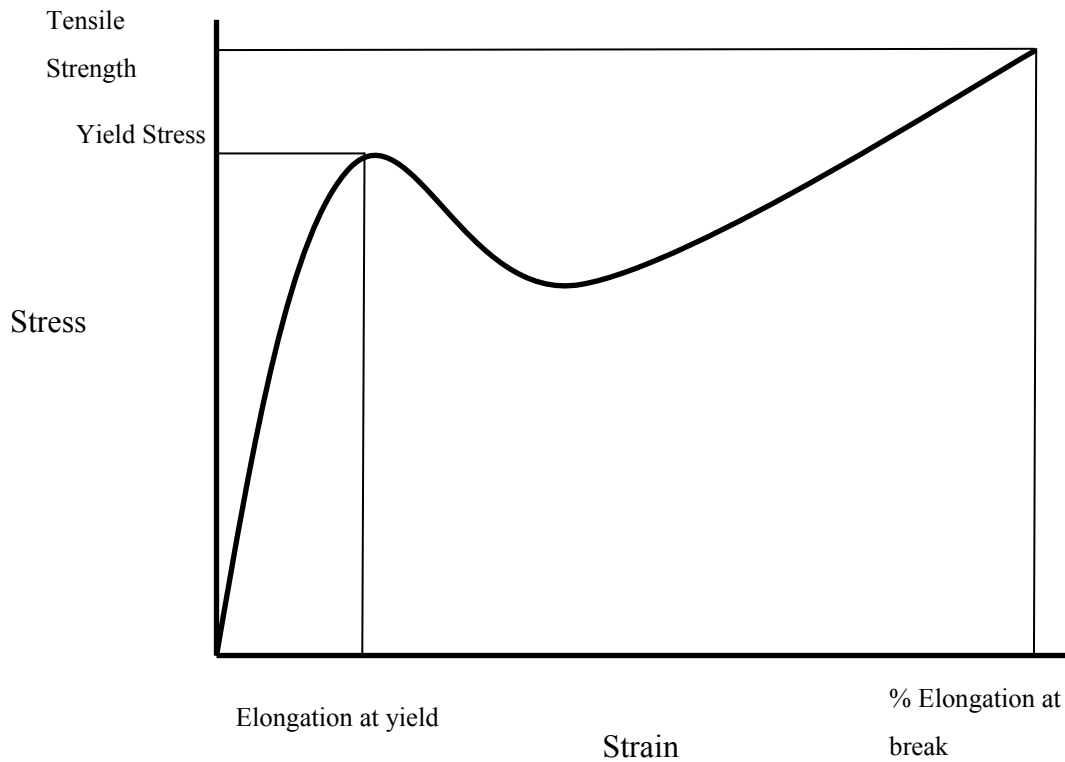
slowly at room temperature to avoid damage. To fast drying makes the films extremely brittle and they tend to crack on the casting plate. The drying time depends on the thickness of the film as well as environmental factors such as temperature and relative humidity. The film thickness depends on solution concentration, dispenser height, and casting speed. Typically large batches of homogeneous films are produced for scientific comparison.

## **Properties**

### ***Mechanical Properties***

Mechanical behavior from a polymers can be evaluated by its stress-strain characteristics under tensile deformation (Selke et al., 2004). Pulling a film can help determine how the material will react when forces being applied in tension. The material's strength along with the amount of % elongation can be measured.

According to Hooke's law, the strain of an elastic material is proportional to the observing stress. The stress- strain curve reveals information about the deformation of a material. The stress is defined as the force applied over an area and the strain is the deformation compared to the dimension of the sample.



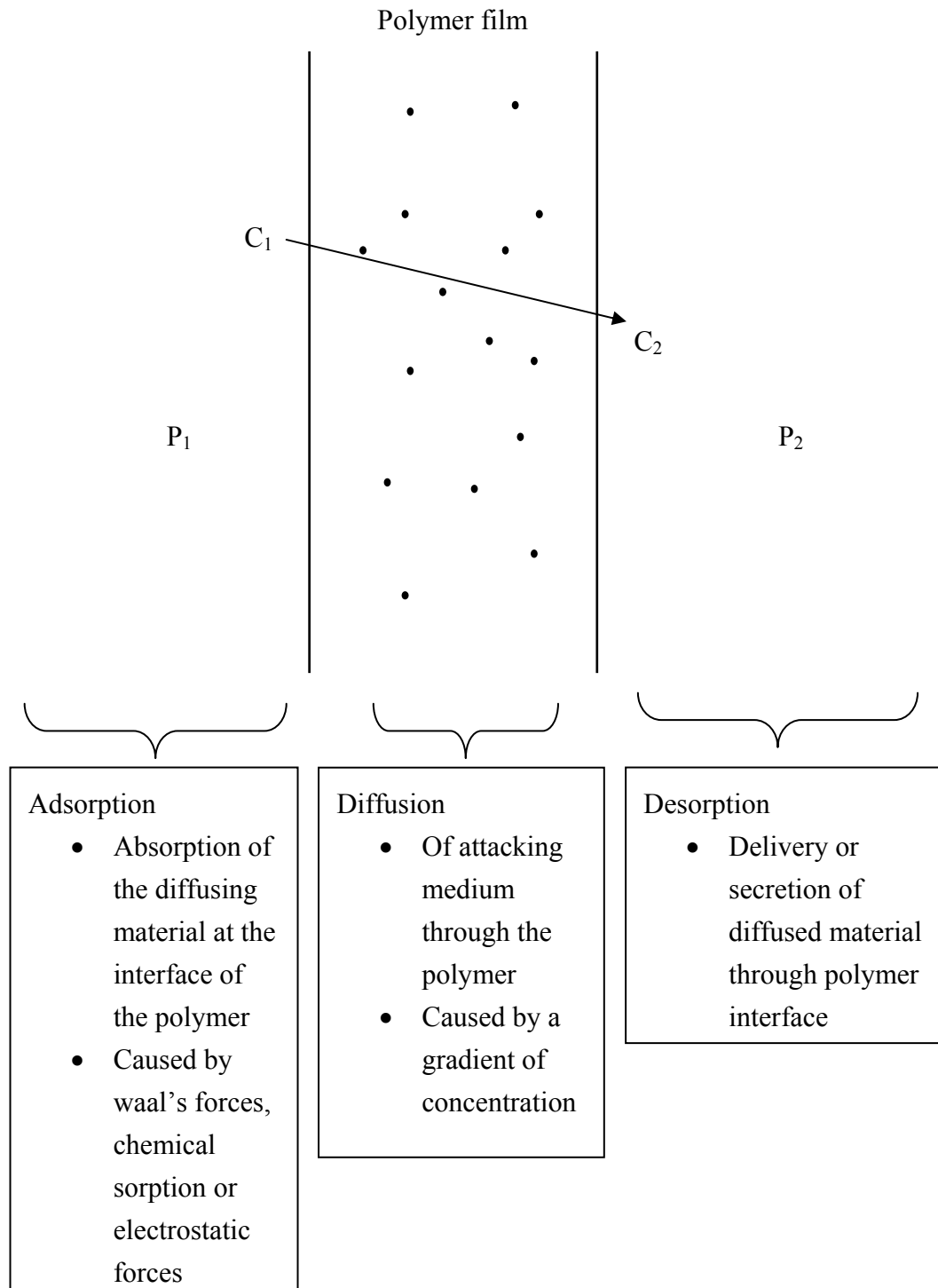
**Figure 9: Stress-Strain curve**

Figure 9 shows a stress- strain curve of an elastic polymer since elongation recovers over time. Brittle polymers, on the other hand, show stress-strain curves that illustrate low EBs. The deformation curves of these polymers do not recover.

***Barrier Properties***

“Barrier properties [of polymers] indicate their resistance to diffusion and sorption of substances” (Selke et al., 2004). Packages with enhanced barrier properties impact the shelf life of products. Enhanced barrier properties include good oxygen and water vapor

permeation since those are the two common barrier concerns in connection with product degradation (Soroka, 1999). “Permeation is the movement of gases, vapors or liquids (called permeates) across a homogeneous packaging material” (Selke et al., 2004). The transmission of gas or vapor through a film can be described as the gas or vapor dissolving at the surface on the film, and evaporating from the other surface at the low concentration (i.e. low-pressure). The material transport through a polymer is summarized in Figure 10. Material transport can only occur if the polymer is homogeneous with no cracks or voids.



**Figure 10: The material transport trough a polymer film**

Source: Redrawn from Osswald et al, 1996.

The permeability of a material for dilute solutions can be described by Henry's Law:

$$P = D \times S$$

Where: D is the diffusion coefficient

S is solubility coefficient (Osswald et al., 1996)

An example of a polymer with enhanced barrier properties has low permeability of water vapor and oxygen. When the diffusion solubility values (compound that is molecularly mixed with a liquid or solid) are low, the polymer has good barrier properties. A perfect barrier is created when an undesirable molecule or gas is unable to go in and through a polymer layer. As free volume increases in a polymer, it is easier for gas or molecules to penetrate through the polymer. Increased crystallization of a polymer decreases the permeability of gasses and molecules. This is directly associated with the fact that crystalline regions offer less free volume than amorphous regions within the polymer. Crystalline areas are tightly structured where molecules or gas must navigate around. Environmental factors, such as humidity and temperature, also have an impact on the barrier properties of hydrophilic films.

### **Oxygen Permeability Measurement System**

Oxygen Permeability Rate can be determined according to ASTM D 3958 with an oxygen transmission rate testing apparatus. When a film is placed inside a controlled chamber, oxygen is blown on one side of the film and nitrogen on the other. The mechanism consists of an inside and outside chamber (see Figure 11). Prepared samples



need to be clamped between the chambers within a diffusion cell, that has been purged of oxygen. Nitrogen is used a carrier gas which routes to the sensor. When oxygen is released, it is allowed to diffuse through the test specimen where nitrogen gas carries the oxygen to the sensor and the rate of transmission is recorded .

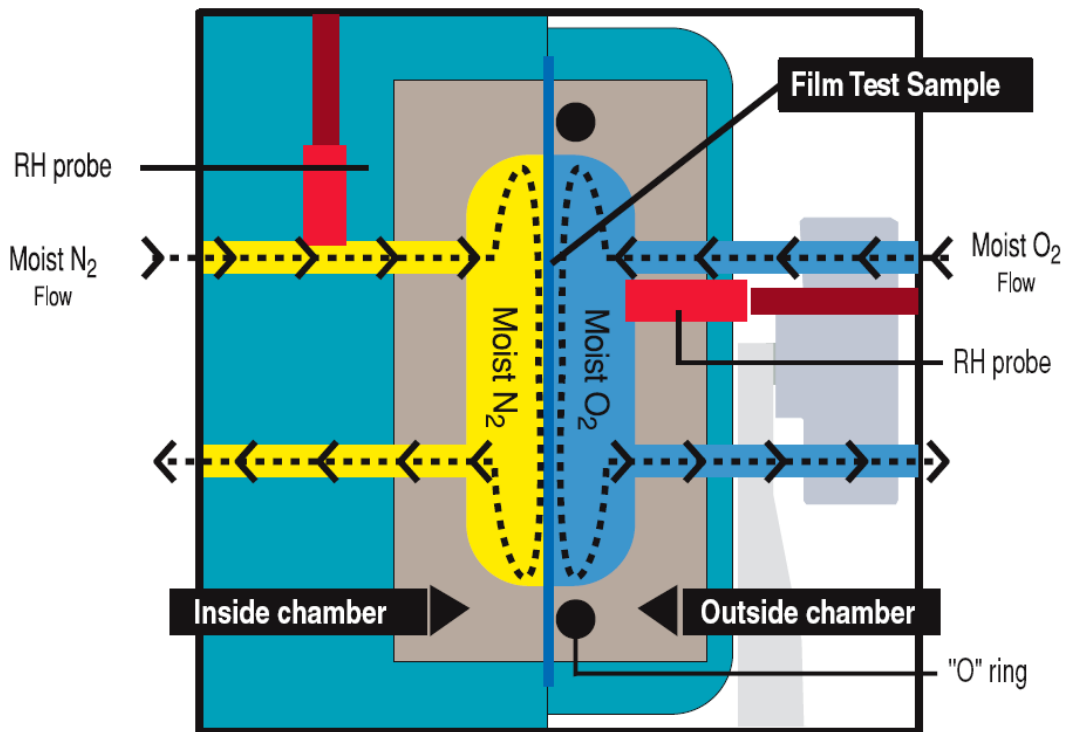


Figure 11: Oxygen Transmission Rate Testing Apparatus

Source: Instruction Manuel Ox-Tran Model 2/21

### Water Vapor Permeability

One of the most common methods to measure water vapor permeability (WVP) through a film is via the gravimetric method (ASTM E96). With this method, water vapor

transmission rates (WVT) of a film can be determined.

**Table 6: Definition WVT and WVP.**

| <b>Acronym</b> | <b>Definition</b>  |
|----------------|--|
| WVT            | the steady water vapor flow in unit time through unit area   |
| WVP            | the time rate of water vapor transmission through unit area of unit thickness induced by unit vapor pressure difference between two surfaces |

The gravimetric method determines the rate of vapor movement through the film by recording the weight of test dishes filled with distilled water over a time. Three test specimens of each sample should be tested. Distilled water is poured in a test dish (impermeable to water or water vapor) to a level  $\frac{3}{4} \pm \frac{1}{4}$  below the test film. The test film must be sealed on the test dish in a controlled temperature and humidity chamber for two hours, in order for the test film to reach a steady state of equilibration before measurements are recorded. The test dish must be weighed in at least eight equal intervals.

**Table 7: Water Vapor Transmission calculation**

|                     |                          |
|---------------------|--------------------------|
| <b>Equation</b>     | $WVT = G/tA = (G/t)/A$   |
| <b>Variable G</b>   | Change in weight         |
| <b>Variable t</b>   | Time when G occurred     |
| <b>Variable G/t</b> | Slope of a straight line |
| <b>Variable A</b>   | Test area                |

**Table 8: Water Vapor Permeance calculation**

|                                       |   |
|---------------------------------------|---|
| <b>Equation</b>                       | $WVT/\Delta p = WVT/ S (R_1 - R_2)$                         |
| <b>Variable <math>\Delta p</math></b> | vapor pressure difference                                   |
| <b>Variable S</b>                     | saturation vapor pressure at test temperature               |
| <b>Variable <math>R_1</math></b>      | relative humidity at the source expressed as a fraction     |
| <b>Variable <math>R_2</math></b>      | relative humidity at the vapor sink expressed as a fraction |

To calculate the water vapor permeability (WVP), the permeance is multiplied by the thickness of the specimens (ASTM E96). Since the ASTM E96 is designed for hydrophobic polymers, it may not apply for hydrophilic film systems. Thus, the modified procedure for WVP (described by Mc Hugh et al., 1993) can be used for hydrophilic films. The correction method is designed for accounting the water vapor partial pressure gradient in the stagnant air layer of the test cups (see Figure 12).

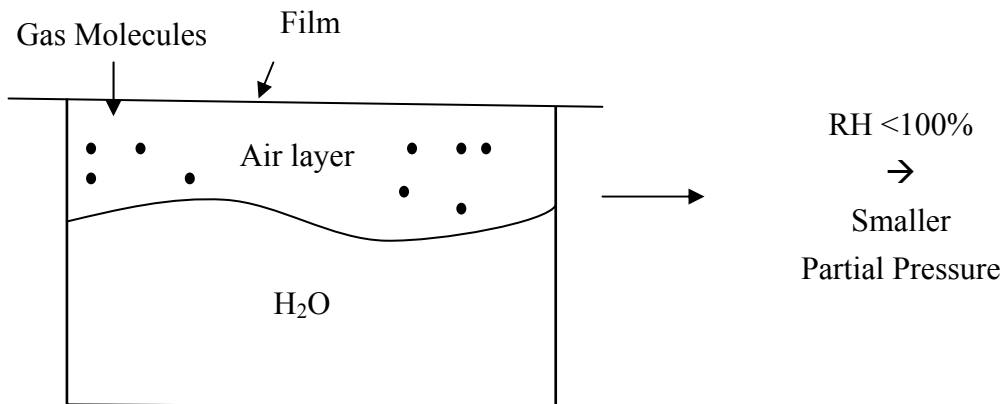


**Figure 12: Stagnant air layer in test dish for WVP (ASTM E96)**

The ASTM method is based on the assumption that the relative humidity under the film in the test cups is 100% (because resistance to mass transfer is negligible). However, the relative humidity below the test film is less than 100% due to a stagnant air layer. The hydrophilic polymer matrix has a greater affinity to water vapor than hydrophobic films. Water molecules are better attracted to the hydrophilic film and absorbed easier than in a hydrophobic film, thus causing fewer molecules to stay under the film. This lowers the relative humidity under the film layer by a greater amount than for hydrophobic films. The mass transfer is therefore different compared to a hydrophobic film. Based on the ASTM standard, the permeation through the film would not account for the stagnant air layer. Therefore, not applying the correction method can yield results that can be off by as much as 35% (McHugh et al., 1993).

## ***Optical characterization***

### **Color and Haze**

The optical appearance of a film may be tested to determine the influence of clay on the visual appeal of the film. To determine the overall appearance of a specimen, haze and color values must be obtained.

Haze is the cloudy or turbid aspect or appearance of an otherwise transparent specimen caused by light scattered from within the sample or from its surface (ASTM D 883). The higher the haze value, the more cloudy (less transparent ) the film becomes. The calculation of Haze is depicted in Table 9.

**Table 9: Calculation Haze**

| <b>Variable</b> | <b>Definition</b>   |
|-----------------|---|
| Haze            | $Y \text{ Diffuse Transmission} / Y \text{ Total Transmission}$ |

L, a, and b values illustrate the color of a specimen, and can be mathematically transferred into the color difference of specimen. Table 10 details color difference.

**Table 10: Calculation of Color Difference**

| <b>Variable</b>                 | <b>Definition/Equation</b>                     |
|---------------------------------|--|
| L-value                         | shows the psychometric lightness               |
| a-value                         | red (+) green (-) axis                         |
| b-value                         | Yellow (+) – Blue (-) axis                     |
| Color Difference ( $\Delta E$ ) | $(\Delta L^2 + \Delta a^2 + \Delta b^2)^{0.5}$ |
| $\Delta L$                      | $L_{\text{sample}} - L_{\text{standard}}$      |
| $\Delta a$                      | $a_{\text{sample}} - a_{\text{standard}}$      |
| $\Delta b$                      | $b_{\text{sample}} - b_{\text{standard}}$      |

Source: Hunter Lab, Software 3.2

### *Microstructural Analysis*

#### **X-Ray Diffraction**

X-Ray diffraction is a commonly used technique to describe the structure of clay minerals and their crystal structures. It is a non-destructive method and only small material specimens are required for testing. Every crystalline structure has its own characteristic atomic structure which diffracts X-ray beams in a characteristic pattern. These patterns present information concerning the type of clay and the distance between the silicate layers. X-Ray diffraction works by exposing X-Ray beams on a specimen. Electrons within a crystal in the path of an incident X-Ray beam (i.e. electrons in the silicate layer) resonate. Each electron periodically absorbs energy from the X-Ray beam, and emits X-radiation of an identical frequency. This diffracted radiation is then recorded as a pattern of angles (see Figure 13). The recorded angles may be transformed into a ‘basal spacing’ using the principle of Braggs Law (Brown, 1961).

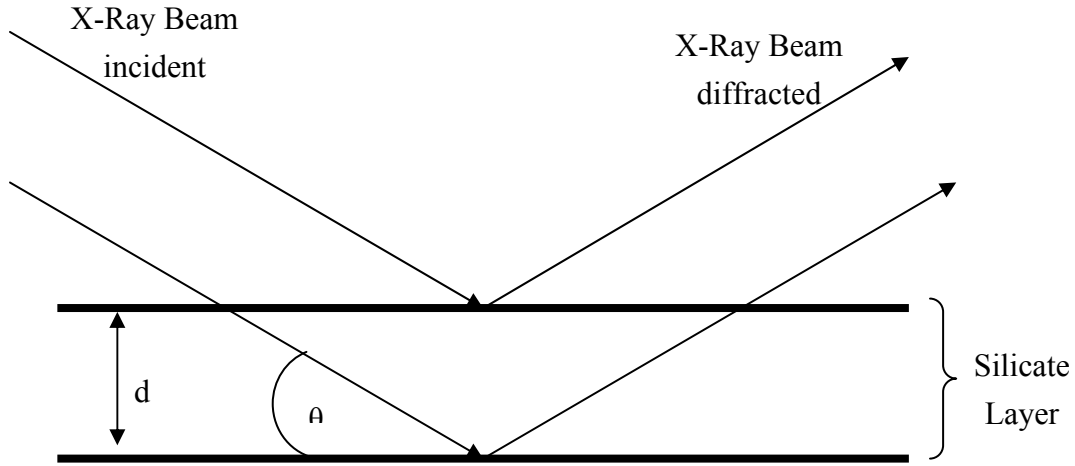


**Figure 13: Explanation Bragg's Law**

Source: Redrawn Brown, 1961

The incident beam meets the silicate layer and is diffracted in a unique pattern. The further apart the silicate layers, as higher the distance between the silicate layers. Following Bragg's Law, the basal spacing of the silicate layers can be calculated using following formula.

$$\text{Bragg's Law: } 2 d \sin \theta = n \lambda$$

**Table 11: Variable Bragg's Law**

| Variable  | Definition/Equation          |
|-----------|------------------------------|
| $\lambda$ | Wavelength                   |
| $\theta$  | glancing angle of reflection |
| N         | Order of reflection          |
| D         | Lattice spacing in Angstrom  |

The calculated spacings resulting from X-Ray diffraction are excellent ways to compare

different crystal structures (Rule et al., 2002 and Brown, 1961). For instance, Cloisite Na<sup>+</sup> has a basal spacing of 11.7 Angstroms and can be compared to the layer distance of clay composite films.

It is expected that the angles for intercalated silicate layers will be lower than pure Cloisite Na<sup>+</sup>, thus will have an increased layer distance. If the X-Ray pattern shows no characteristic angle peak, no basal distance can be calculated and it can be noted that the clay layers are exfoliated.

## **TEM**

Transmission Electron Microscopes (TEM) are designed for high standard atomic resolution imaging and chemical analysis. There are two fundamental physical concepts based on the TEM technique. First, the moving electrons can be assigned to very short wave lengths (different to the wavelength of light). Second, electrostatic or magnetic fields can be used as true lenses for producing an enlarged image (Wischnitzer, 1962). To obtain high resolution images, the samples must be prepared carefully. The specimen needs to be cut into nanometer thick samples, because the picture is taken through a cross-section of the film. The samples are then placed on a copper grid in the microscope. The samples are fired with electrons with a focused electron beam. The images appear on a phosphor screen below the specimen and are transmitted to the computer screen. The TEM uses electrons which are fired through an electron gun. The condenser lens focus the electron beam on the specimen and provides an optically illuminating condition for



visualizing and recording the image. An enlarged image of the specimen is formed by the objective lens, which is projected on the screen by the projector lens (Figure 14).

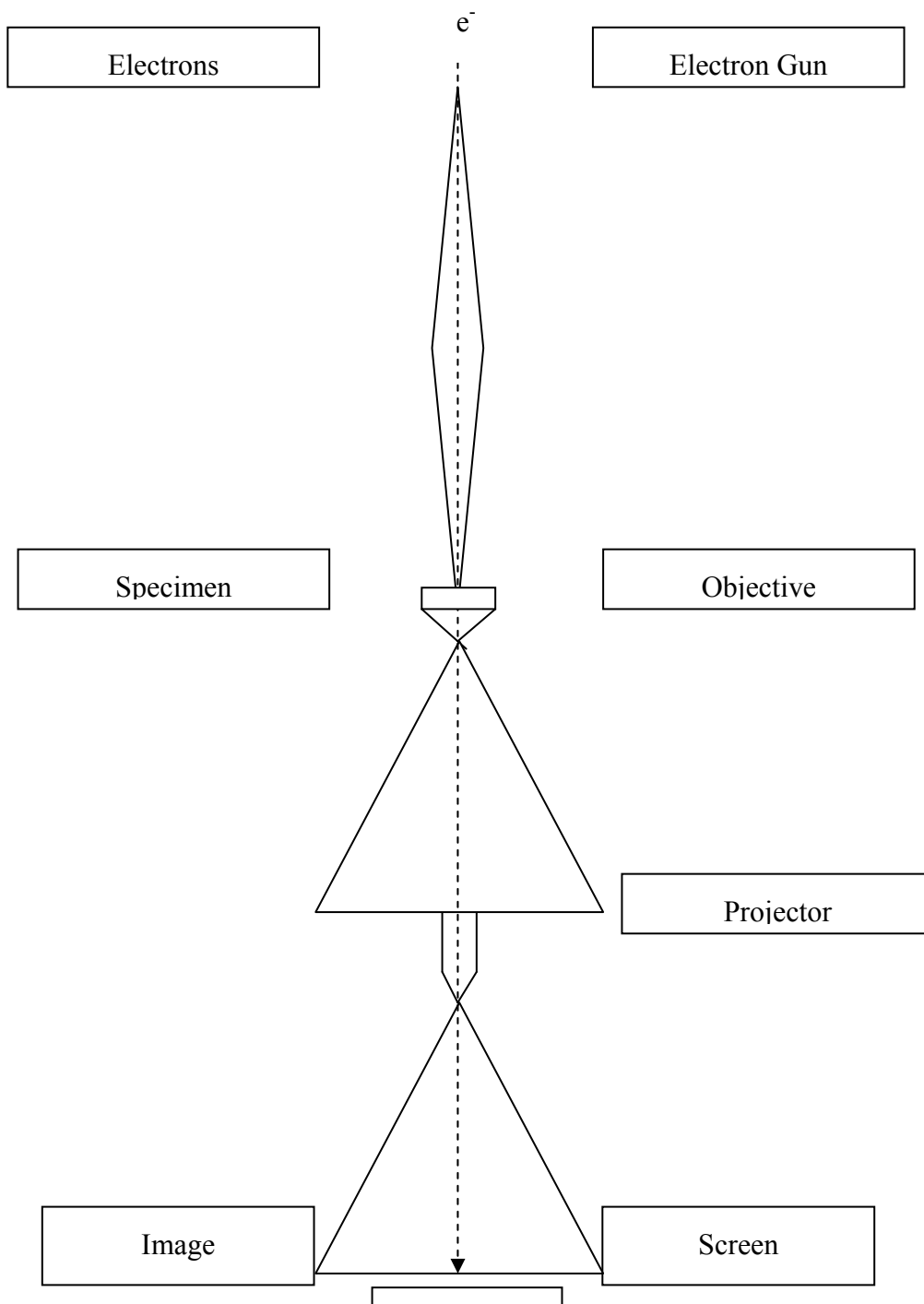


**Figure 14: Method of operation of TEM**

Source: Redrawn from Wischnitzer, 1962 and Brandon et al., 1999.

## CHAPTER THREE

### III EXPERIMENTAL DESIGN

#### Materials

Mung Bean Starch was obtained from HAITAI Inc. (Montebello, CA). The natural unmodified montmorillonite clay (Cloisite Na<sup>+</sup>) used was produced by Southern Clay Products with a layer distance  $d_{001}$  of 11.7 Å. Glycerol was obtained from Mallinckrodt Baker, Inc. (Phillipsburg, NJ).

#### Methods

The pure starch films were produced by combining 9% of mung bean starch, 25% wt of glycerol and degassed distilled water. The solution was constantly stirred and heated in the water bath (Haake, Model FE2, Saddle Brook, NJ, USA). After reaching 95 °C, the gelatinized solution was observed for bubbles which were removed by suction. The solution was cast on a flat, clean casting plate. Film needed to dry under room temperature for 32 hours. The dried films were separated from the casting plate (BYTAC, Norton Performance Plastics Corporation, Wayne, NJ, USA) and cut into test specimens.

The starch composite films were produced by mixing 9% starch with distilled, degassed water. Similarly, clay, 25% wt glycerol and distilled, degassed water were combined in a different cup. This solution was ultrasonified with a Branson sonifier (Model S450D). The starch mixture was heated in the water bath. The ultrasonified clay mixture was

slowly combined with the starch mixture. Under continuous stirring and heating, the temperature was increased to 95°C and the gelatinized mixture was cast on a flat and clean casting plate. The film was allowed to dry for 32 hours under room temperature (23 °C).

The water bath had to be modified with an additional water heater to reach the correct temperature of 95°C. The mixture was stirred in polypropylene cups with a weight on top to secure the position in the water bath. A additional silicon tube was installed in the water bath to insure consistent temperature and water flow in all areas of the water bath. The water bath and the polypropylene cup were covered with aluminum foil to avoid evaporation of water and to maintain the temperature of the water. The process of degassing water was critical to produce a high quality film. Only with degassed water can air bubbles be eliminated from the film. The distilled water was degassed for at least 5 hours before use. To maintain a homogeneous thickness and properly cast the film, starch concentration and casting speed were considered. The best starch concentration was found to be at 9%. Less starch resulted in low gelatinizing which yielded a poor film. Films with higher starch concentrations were prone to air bubbles due to the high gelling rate that retarded the movement of air from the mixture.

The film solution was cast with a film applicator (PI-1210 Filmcoater, Tester Sanggyo CO., LDT, Tokyo, Japan) onto a BYTAC (Norton Performance Plastics Corporation, Wayne, NJ, USA) which was coated on a glass plate. The casting speed, distance

between the casting plate and the casting suspender were also considered. A low casting speed (i.e. 25mm/sec) resulted in specimens that were too thick and cracked while drying (Figure 15). A fast casting speed (50 mm/sec) resulted in damaged and broken films. The optimal casting speed for producing a film was determined to be 35 mm/sec with an optimal casting distance of 0.381 mm. The ends of each casted and dried film were removed for testing due to the variation in film thickness.



**Figure 15: Film cracking due to low casting speed**

### **Composition Batches**

Two main production batches of film were produced for all testing. Each main batch was produced on one day under same conditions. All batches contained 9% starch. The ultrasonification batch contained a consistent amount of 5% clay and 25% plasticizer.

The influence of different ultrasonification times of the clay on film properties was determined. The ultrasonification batch produced six separate batches that yielded five cast films per batch, for a total of 30 films (Table 12).

**Table 12: Ultrasonification Batch Identification**

|                           | <b>Batch<br/>1</b> | <b>Batch<br/>2</b> | <b>Batch<br/>3</b> | <b>Batch<br/>4</b> | <b>Batch<br/>5</b> | <b>Batch<br/>6</b> |
|---------------------------|--------------------|--------------------|--------------------|--------------------|--------------------|--------------------|
| ID                        | S0C0               | S0C5               | S5C5               | S10C5              | S30C5              | S60C5              |
| Starch Content            | 9%                 | 9%                 | 9%                 | 9%                 | 9%                 | 9%                 |
| Glycerol Content          | 25%                | 25%                | 25%                | 25%                | 25%                | 25%                |
| Clay Content              | 0%                 | 5%                 | 5%                 | 5%                 | 5%                 | 5%                 |
| Ultrasonification<br>Time | 0 min              | 0 min              | 5 min              | 10 min             | 30 min             | 60min              |

It was determined that a ultrasonification time of 30 minutes was optimal for film properties (see Results section). A second batch was created that produced films with different amounts of montmorillonite clay. This batch was used to determine the influence of clay content on the composite films. Seven different sample batches with clay content between 0 and 30% (wt) were produced and labeled (Table 13).

**Table 13: Clay Batch Identification**

|                             | <b>Batch</b> | <b>Batch</b> | <b>Batch</b> | <b>Batch</b> | <b>Batch</b> | <b>Batch</b> | <b>Batch</b> |
|-----------------------------|--------------|--------------|--------------|--------------|--------------|--------------|--------------|
|                             | <b>1</b>     | <b>2</b>     | <b>3</b>     | <b>4</b>     | <b>5</b>     | <b>6</b>     | <b>7</b>     |
| ID                          | S0C0         | S30C5        | S30C10       | S30C15       | S30C20       | S30C25       | S30C30       |
| Starch<br>Content           | 9%           | 9%           | 9%           | 9%           | 9%           | 9%           | 9%           |
| Glycerol<br>Content         | 25%          | 25%          | 25%          | 25%          | 25%          | 25%          | 25%          |
| Ultrasonifi-<br>cation Time | 30 min       | 30 min       | 30 min       | 30 min       | 30 min       | 30 min       | 30 min       |
| Clay<br>Content             | 0%           | 5%           | 10%          | 15%          | 20%          | 25%          | 30%          |

For comparison, a third batch of films was produced to determine the influence of longer ultrasonification times. For this batch, a ultrasonification time of sixty minutes was applied to a composite containing 10 % nanoclay.

**Table 14: Composition Batch S60C10**

|                        | <b>Batch</b> |
|------------------------|--------------|
| ID                     | S60C10       |
| Starch Content         | 9%           |
| Glycerol Content       | 25%          |
| Ultrasonification Time | 60 min       |
| Clay Content           | 10%          |

## **Methods**

After producing the composite films, mechanical and barrier properties were tested to record how ultrasonification times and percent clay affect the properties of mung bean composites. TS and EB were determined by testing 10 specimen per batch. Water vapor permeability was determined on 3 films from each batch. Oxygen Permeability was tested on two representative test specimens for each batch. X-Ray Diffraction was conducted for 3 films from each batch. All test specimens were compared to a control mung bean film sample.

## Statistical Analysis

The statistical analysis was performed using ANOVA procedures. The analysis was conducted using SAS software (version 9.0, SAS Institute Inc., Cary, NC, USA) and



differences of the means were processed by Duncans multiple range test. The defined significance level was set to  $P < 0.05$ .

### Tensile Properties

The tensile properties were measured according to ASTM D882 standard test method for “Tensile Properties of Thin Plastic Sheeting” on an Instron Universal Testing Machine (Model 4201, Instron Corp., Canton, MA, USA). Tensile Strength is the maximum stress a material can sustain when applied by a force. It is calculated by dividing the maximum load by the cross sectional area of the specimen. The size of the film were cut into 2.54 x 10 m specimen. Samples were conditioned for 48 hours at 23°C and 50% RH. % Elongation at Break is defined as the percentage elongation at the moment of rupture of the test specimen. EB is obtained by dividing the extension by the gage length of the sample and multiplying by 100. 10 specimens of the size of 2.54 x 10 cm were tested for each batch and conditioned for two days under 23°C and 50% RH.

The specimens were conditioned for 48 hours in a constant temperature and humidity chamber (Model TR-001-1, Jei Tech Co., Ltd., Korea) before TS and elongation properties were determined. Initial grip separation was set at 5cm and cross-head speed was set to 12.5 mm/min.

### Oxygen Permeability

Oxygen permeability was determined on two samples for each produced batch. Samples were prepared and tested in the Illinois 8001 Oxygen Permeation Analyzer (Model 8001, Illinois Instruments, Inc., Johnsburg, Illinois, USA). The procedure required ~ 24 hours per sample. The chamber was conditioned to 23 °C at 50% relative humidity (RH). The oxygen transmission rate (OTR) was recorded in cc/m<sup>2</sup>/day. To calculate the permeability of the specimen, the respective OTR was multiplied by the thickness of the film. For permeability testing, the thickness of each film was measured immediately after releasing from the diffusion cell using a digital micrometer (ID-C112, Mitutoyo Corp., Kawasaki, Kanagawa, Japan).

### Water Vapor Permeability

The WVP of the film was determined gravimetrically at 23 degrees Celsius at 50% RH using ASTM E96-93 cup method. For each batch, 3 films were tested. The procedure was conducted in two days. Sample cups were filled with 18ml distilled water and test specimens were sealed on the cup using a rubber gasket. The samples were placed in a constant temperature and humidity chamber (Model TR-001-1, Jeio Tech Co., Ltd., Korea) and conditioned for two hours before use. The WVP values were calculated by using the WVP correction method (Genadios, et al). Three samples for each batch were prepared, and the weight loss as a function of time was recorded once per hour for eight hours.

### Color and Haze

The Haze and color (L, a, and b) values were measured using a ColorFlex 45/0 Spectrophotometer with Universal Software version 3.73 (Hunter Associates Laboratory, Inc., Reston, Va, USA). A white standard plate (No. C6664) was used for calibrating the machine. The color of each film from every batch was measured three times in different positions. The average values were compared to the standard starch film without any clay.

### X-Ray Diffraction

The X-Ray Diffraction was measured on a XDS 2000 Scintag Diffractometer operating at 30.0 mA, 40.0 kv and 1.2 kW to indicate the dispersion of the clay silicate layers. A diffractogram was recorded between  $2\theta$  angles of  $2^\circ$  and  $10^\circ$ .

### Transmission electron microscopy

TEM images were obtained to confirm X-ray pattern results with a H-9500 TEM (HITACHI, Japan).

## CHAPTER FOUR

### IV. RESULTS AND DISCUSSION

In order to investigate the dispersion of Cloisite Na<sup>+</sup> clay in the matrix, an X-Ray diffraction analysis was performed on the composite films.

#### X-Ray Diffraction\

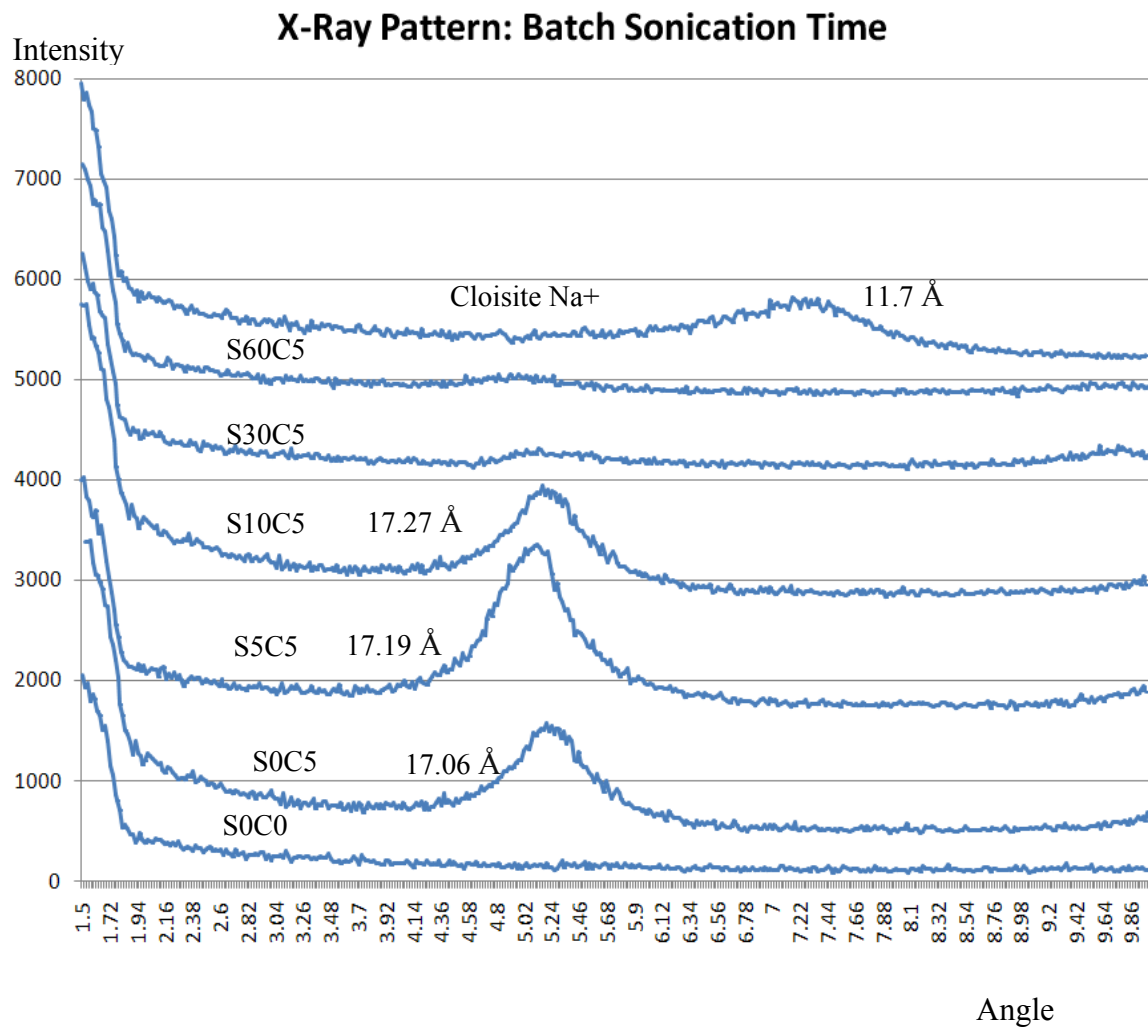
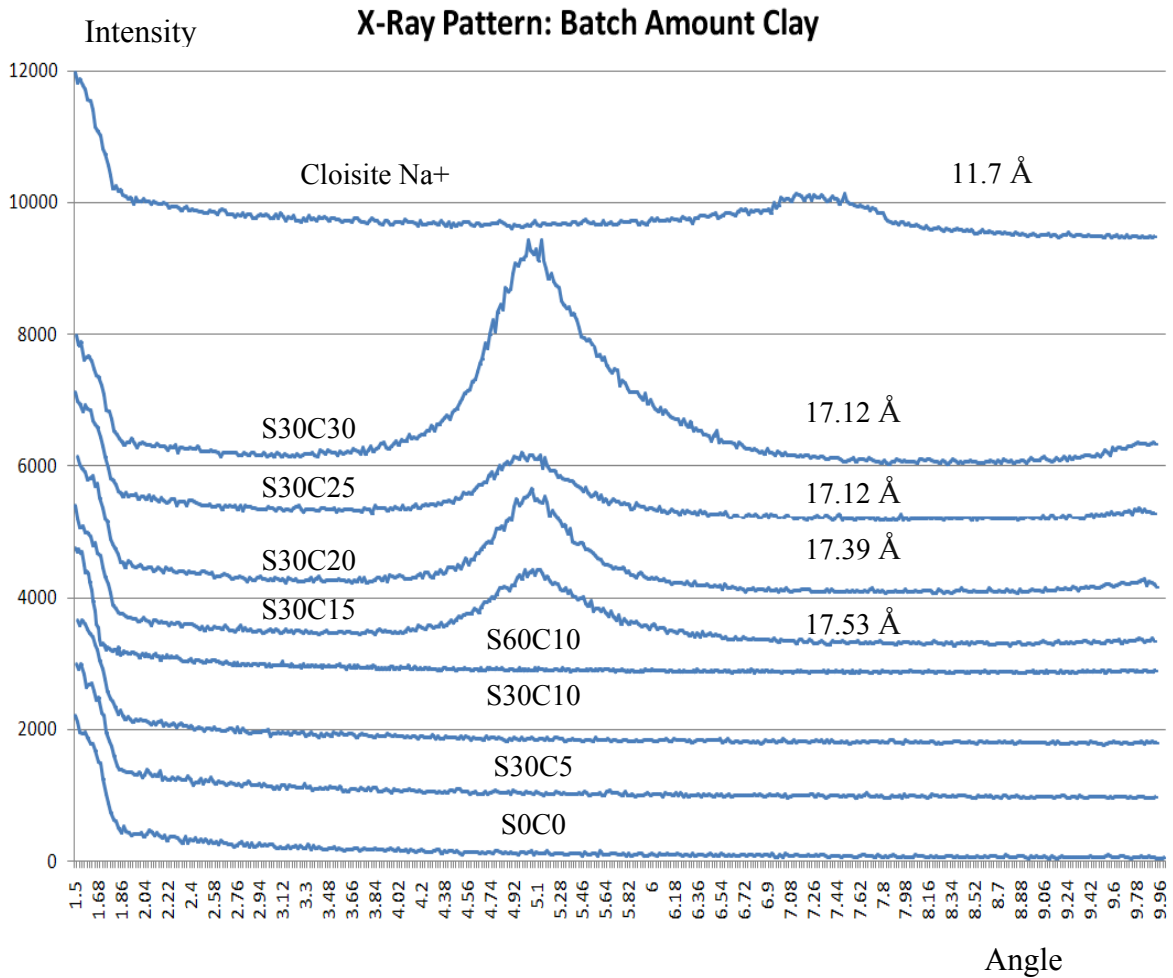


Figure 16: X-Ray Pattern, Batch Ultrasonification Time

Figure 16 shows the pattern obtained for pure clay Cloisite Na<sup>+</sup> and the ultrasonified montmorillonite mung bean composite films. Cloisite Na<sup>+</sup> shows a characteristic “Bragg Diffraction Peak” between 7 and 8 degrees which refers to a layer distance of 11.7 Å. All the samples ultrasonified for 0, 5 and 10 minutes displayed shifted diffraction peaks towards lower angles with a interplanar distance from 17.06 to 17.26 Å. These results indicate that the polymers entered the silicate sheets forming an intercalated composite film due to the polar interactions between hydroxyl groups of the starch and the clay silicate layers. Samples ultrasonified for 30 and 60 minutes did not show a diffraction peak; indicating successful exfoliation. The results indicate that the dispersion of Cloisite Na<sup>+</sup> clay is affected by ultrasonification time. The best exfoliation results were observed during 30 and 60 minutes of ultrasonification. The optimum ultrasonification time for a 5% clay sample was determined to be 30 minutes.

To determine the clay structure in the composite samples containing increasing clay amounts, X-Ray patterns were observed.



**Figure 17: X-Ray Pattern, Batch Clay Amount**

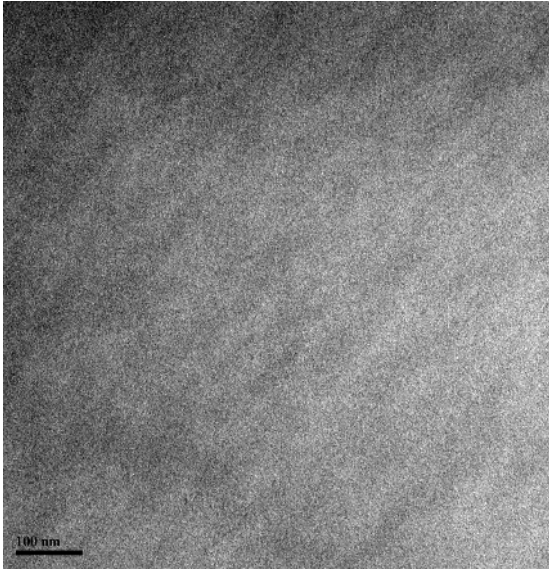
The X-ray patterns for all composite samples were recorded. All samples (Figure 17) show increased dispersion of clay since the interlayer space of Cloisite Na+ increased. This is based on the fact that the reflection angles were smaller and shifted towards the left. Samples with 5 and 10% wt Cloisite Na+ showed an exfoliated structure. It was

observed that achieving full exfoliation became more difficult as the clay level increased. An explanation for this phenomenon could be linked to the solution viscosity. Clay is known to swell in water. With the addition of clay, the solution becomes more viscous, and harder to ultrasonify. Also, it was shown that between 15 and 30% wt clay the peak shifts insignificantly. As clay content is increased in the solution, there is less room for clay to disperse. Previous research has shown that adding clay to high amylase starches made exfoliation difficult. The increase in interlayer separation was limited by the high viscosity of the solution (Mondragon et al., 2008 and Dean et al., 2006).

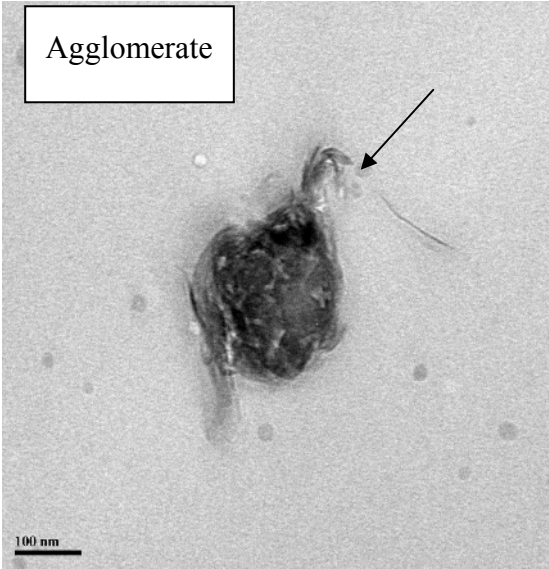
### **Transmission Electron Microscopy (TEM)**

TEM was used to confirm the dispersion of the montmorillonite in the mung bean starch matrix. Image S0C0 shows the mung bean starch control sample without any Cloisite Na<sup>+</sup>. The images of 30 and 60 minute ultrasonified nanocomposites reveal a well dispersed and exfoliated clay matrix. The arrows in the images point to well separated clay layers, supporting the X-Ray Diffraction pattern. Specimens with 5% non-ultrasonified Cloisite Na<sup>+</sup> (S0C5), as well as the image of sample S5C5 show unsatisfactory clay dispersion based on the agglomerates in the matrix. Agglomerates are clay fragments which are fused together. The image of S10C5 is an example of properly intercalated layer structures. The clay silicate layer distances increased from 1.17 nm to 1.73 nm, as the X-Ray pattern reveals, but full exfoliation did not occur. However, some silicate layers are shown to be fully exfoliated.

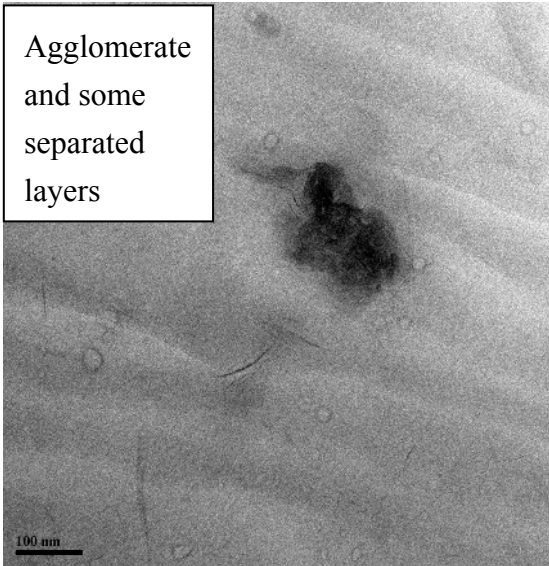
S0C0



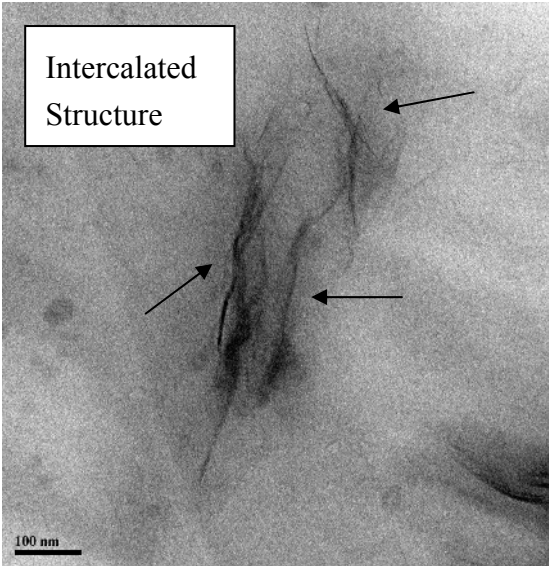
S0C5



S5C5



S10C5





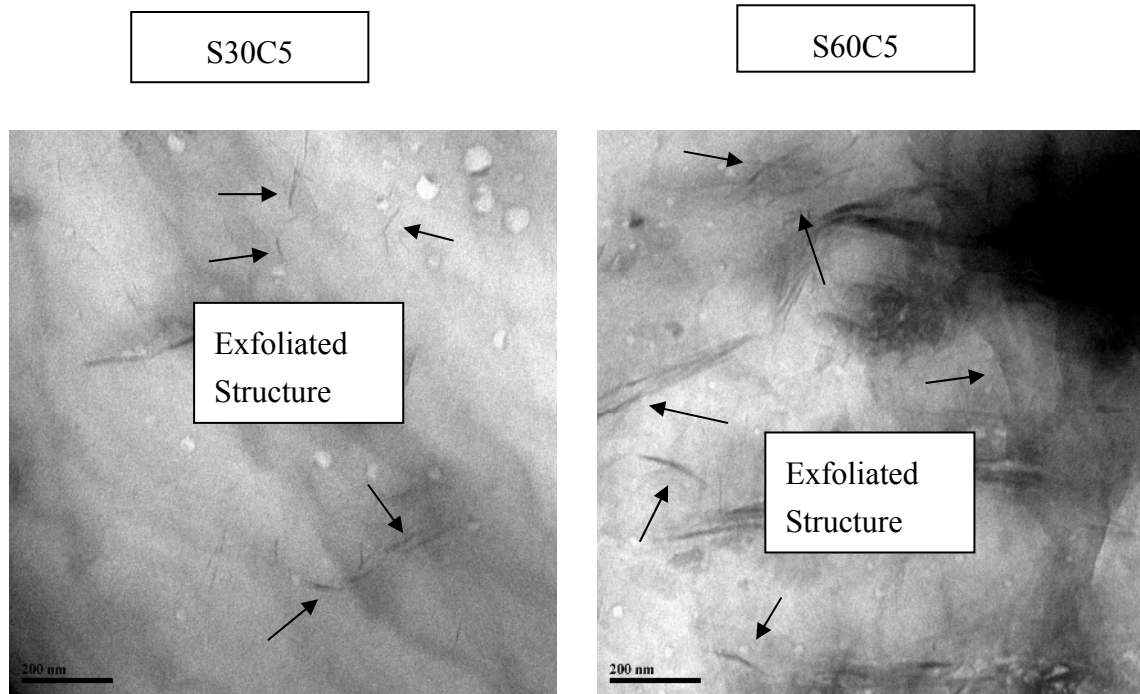
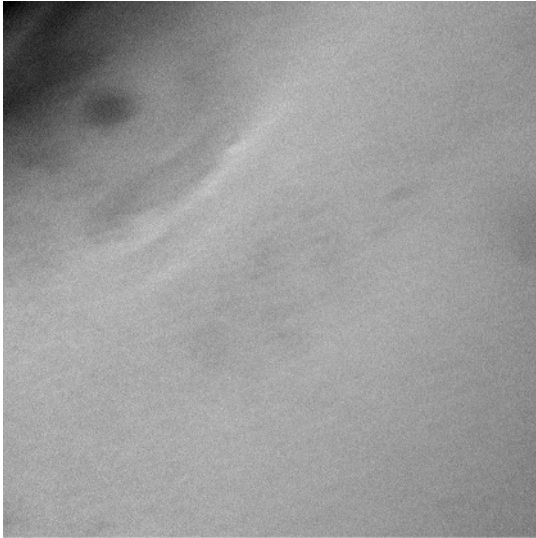


**Figure 18: TEM images, Batch Ultrasonication Time**

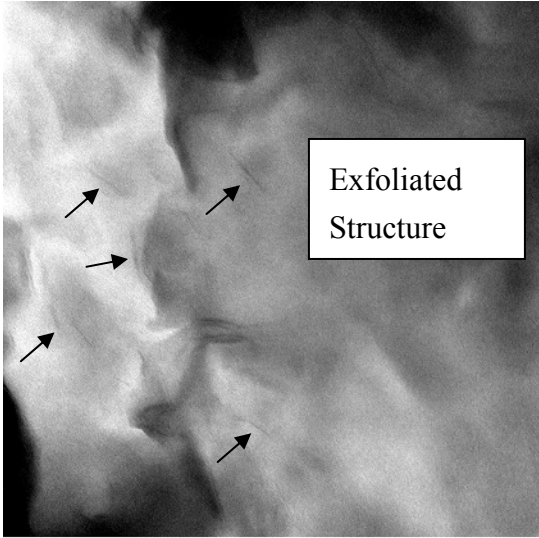
TEM images were also taken for composite films with different levels of clay additions as well as the control. The images also support the results obtained by the X-Ray Diffraction Pattern. The image S0C0 shows the pure starch matrix. Clay film with lower clay additions (5 and 10%) show well exfoliated clay. This is shown by errors pointing on exfoliated silicate layers. The dispersion of Cloisite Na<sup>+</sup> is well distributed through the mung bean starch matrix. With increasing the amount of clay, more intercalated structures are revealed. This is well demonstrated in sample S30C30. Also, the more clay added to the matrix, the more agglomerate parts are seen in images S30C20 and S30C25 . Silicate layer exfoliation can not be seen in the specimens with higher clay content.

S0C0



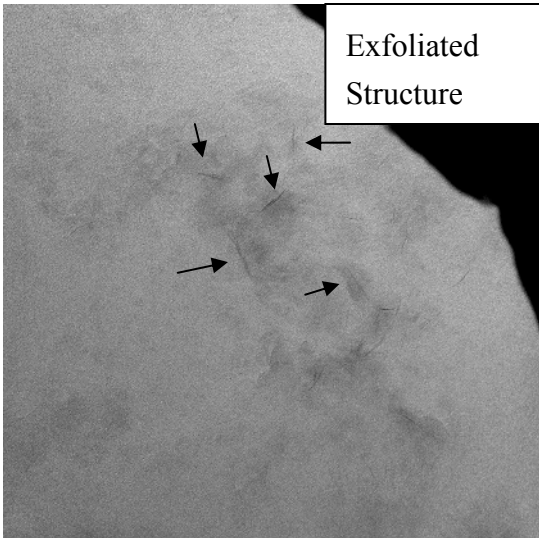
S0C0-01.tif  
S0C0  
Print Mag: 103000x @ 51 mm  
20:49 10/14/08  
TEM Mode: Imaging  
100 nm  
HV=120kV  
Direct Mag: 300000x  
Clemson EM Center

S30C5



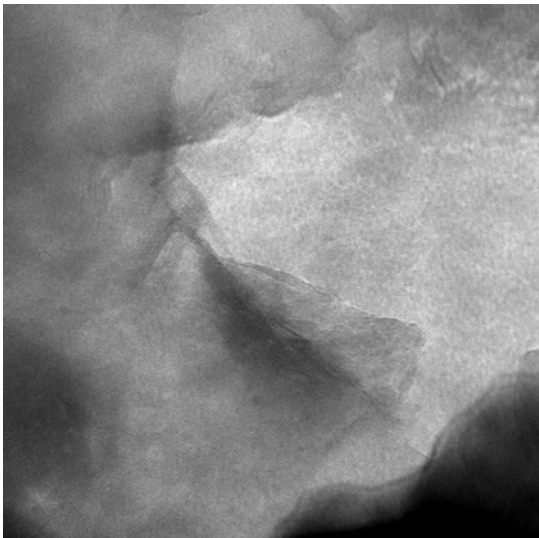
S30C5-04.tif  
S30C5  
Print Mag: 68900x @ 51 mm  
20:24 10/14/08  
TEM Mode: Imaging  
100 nm  
HV=120kV  
Direct Mag: 200000x  
Clemson EM Center

S30C10



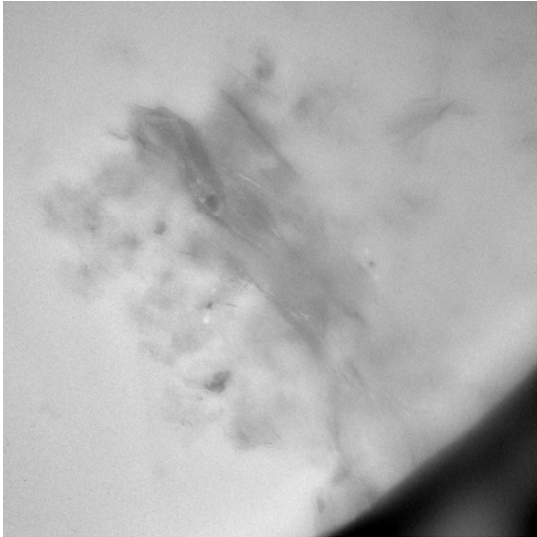
S30C10-04.tif  
S30C10  
Print Mag: 51700x @ 51 mm  
19:03 10/14/08  
TEM Mode: Imaging  
100 nm  
HV=120kV  
Direct Mag: 150000x  
Clemson EM Center

S30C15



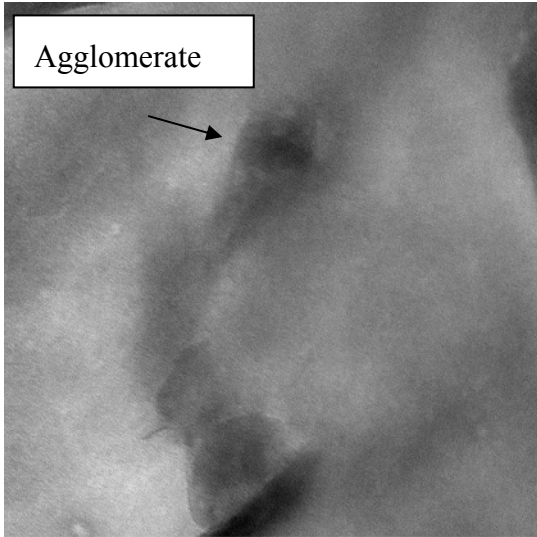
S30C15-02.tif  
S30C15  
Print Mag: 138000x @ 51 mm  
19:15 10/14/08  
TEM Mode: Imaging  
100 nm  
HV=120kV  
Direct Mag: 400000x  
Clemson EM Center

S30C20



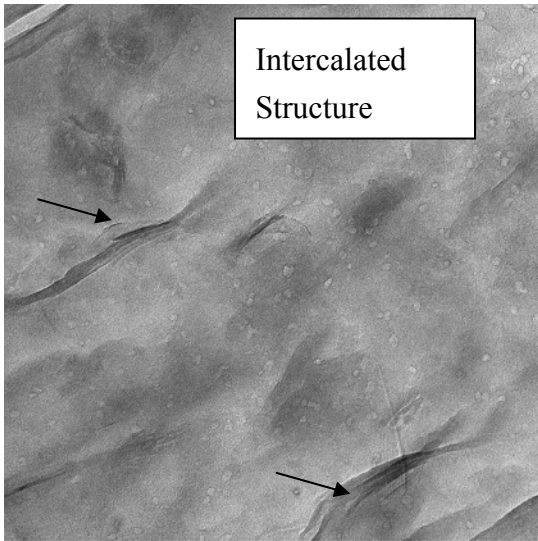
S30C20-02.tif  
S30C20  
Print Mag: 13700x @ 51 mm  
19:57 10/14/08  
TEM Mode: Imaging  
500 nm  
HV=120kV  
Direct Mag: 40000x  
Clemson EM Center

S30C25



S30C25-04.tif  
S30C25  
Print Mag: 103000x @ 51 mm  
20:12 10/14/08  
TEM Mode: Imaging  
100 nm  
HV=120kV  
Direct Mag: 300000x  
Clemson EM Center

S30C30

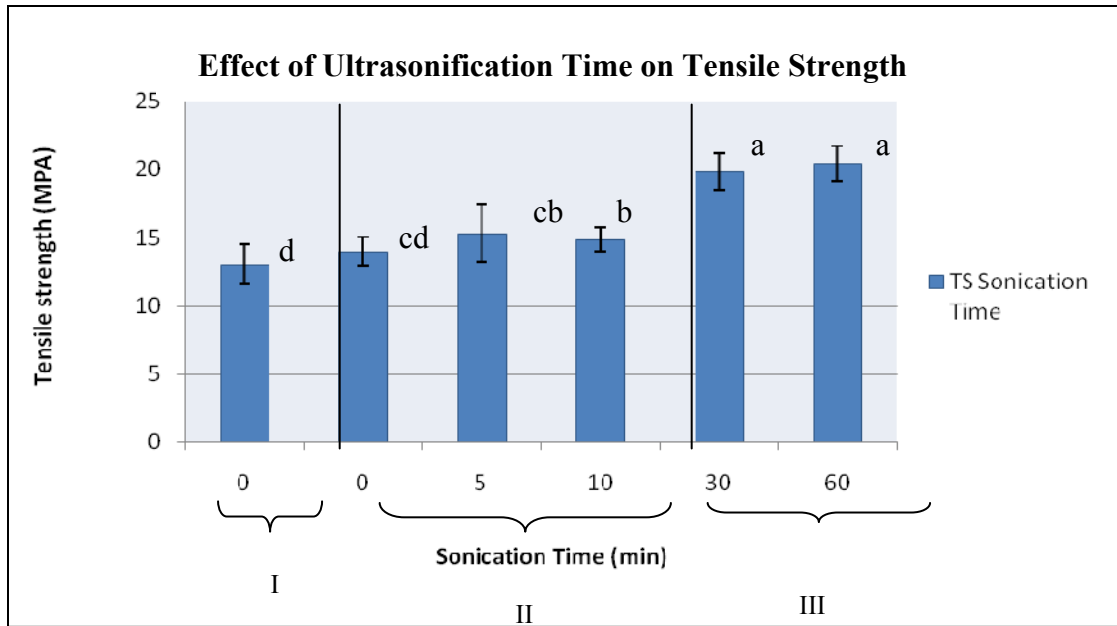


S30C30-02.tif  
S30C30  
Print Mag: 51700x @ 51 mm  
20:32 10/14/08  
TEM Mode: Imaging  
100 nm  
HV=120kV  
Direct Mag: 150000x  
Clemson EM Center

Figure 19: TEM images, Batch Clay Amount

## Tensile Strength

The recorded stress strain data revealed a brittle behavior for starch clay sample films.



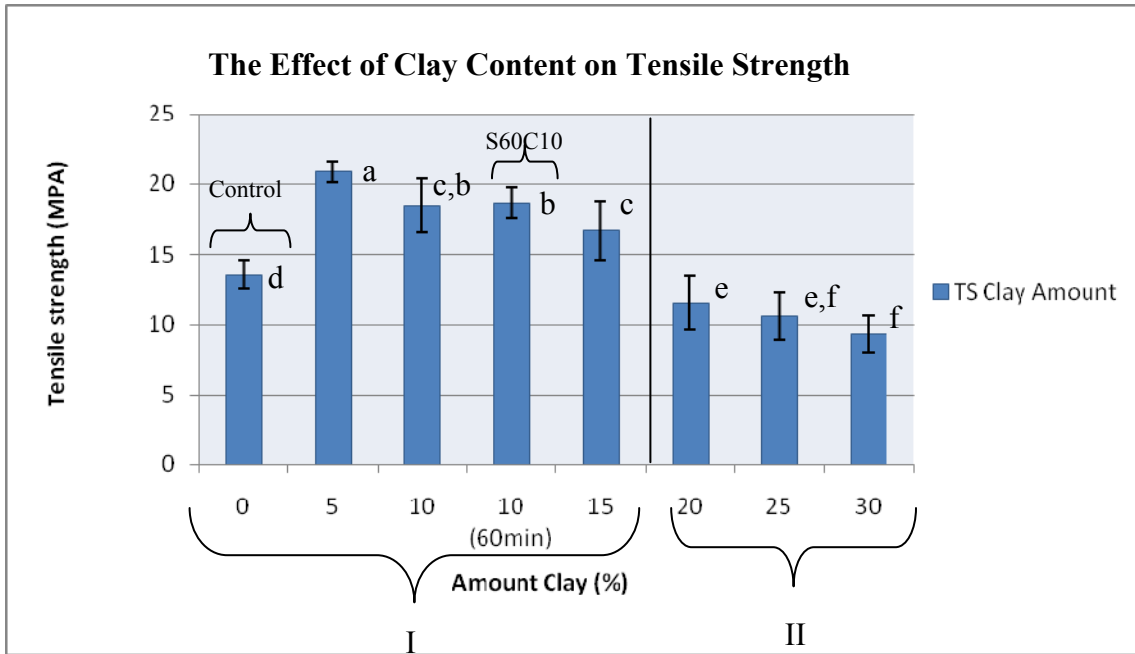
\* Means with the same letter are not significantly different

**Figure 20: Tensile Strength Results, Batch Ultrasonification Time**

Figure 20 illustrates the effects of ultrasonification time on tensile strength. The samples were prepared with 5% Cloisite Na<sup>+</sup> as indicated in Table 12. The TS of starch composite films tends to increase with increasing ultrasonification times. The data in Figure 20 can be grouped into three sections (I, II and III). Section I contains the pure mung bean starch samples with the lowest tensile properties. Section II depicts starch/clay composite samples with improved tensile properties. The non-ultrasonified clay composites show only slight improvement over the control. The tensile properties of composites are constant up to 10 minutes of ultrasonification and reveal greater TS properties than the

control sample. Increased ultrasonification time resulted in increased TS. The highest TS values were obtained for specimens ultrasonified for 30 and 60 minutes (as shown in Section III). Both differ significantly from the control and the low ultrasonified sample values. However, TS values for 30 and 60 minute samples differed insignificantly from each other. Ultrasonification for 30 and 60 minutes increased TS by 57% and 58% respectively.

The improvement of mechanical properties for starch-clay composite films have been attributed to the structure and dispersion of silicate layers in polymer films (Park et al., 2002). The increased TS for the longer ultrasonified composite samples can be attributed to better dispersion of the clay layers in the matrix. The exfoliated film composition includes clay layers which secure a more rigid and crystalline-like structure, thus increasing the TS. Figure 16 depicts the exfoliated clay layers in the matrix. The intercalated clay layers for the remaining composite films show decreased mechanical properties of specimen when treated with lower ultrasonification times. The clay layers in the samples are less dispersed in the film matrix, thereby creating larger amorphous areas which limit optimum TS.



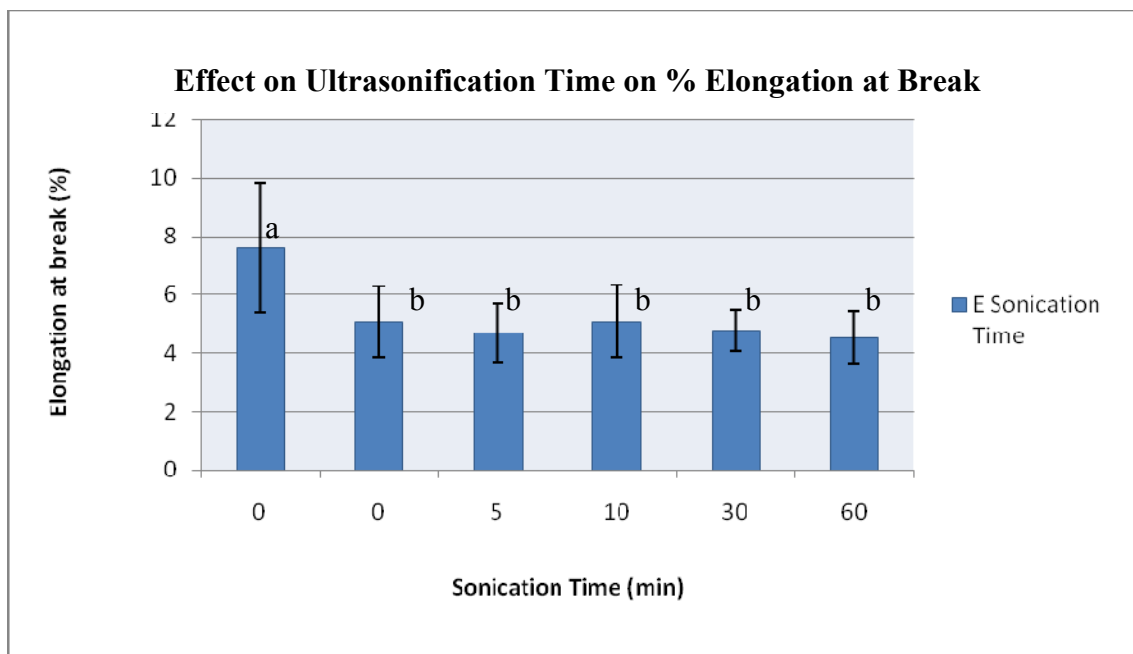
\* Means with the same letter are not significantly different

**Figure 21: Tensile Results, Batch Clay Amount**

Figure 21 shows the effect on tensile strength as percent clay content. The graph can be grouped into two parts. The first part of the graph depicts specimens with 5-15% wt. clay content. Films with 5-15% clay showed a significant improvement in TS, especially S30C5 which had a 54% increase in strength. This improvement is related to excellent dispersion of nanoclay. Interestingly, the TS for higher clay content (>15%) films showed a decrease in TS values. The TS decreased significantly, even lower than the control. This is due to the poor distribution of nanoclay within the mung bean starch matrix. The occurrence of clay agglomerates resulted weak films. TS was decreasing significantly. Clay agglomerates do not support the matrix and create weak areas in the film. Similar results were observed by Kampeerappun (2006). Kampeerappun noted

that the TS for composite films decreased with higher clay contents. It was explained that this phenomena was caused by poor particle distribution of the higher clay content samples. Similar observations regarding the dispersion of clay particles and mechanical film properties were also reported by Pandey (2005). The samples with 10% clay content ultrasonified for 60 minutes showed no difference when compared to the same sample ultrasonified for 30 minutes.

### **% Elongation at Break**



\* Means with the same letter are not significantly different

**Figure 22: % Elongation at Break, Batch Ultrasonification Time**

The EB was determined for the control and ultrasonified composite films. All composites showed lower EB than pure starch films. Composite films compared to each other do not

differ significantly. These results indicate that the ultrasonification time has no influence on the EB.

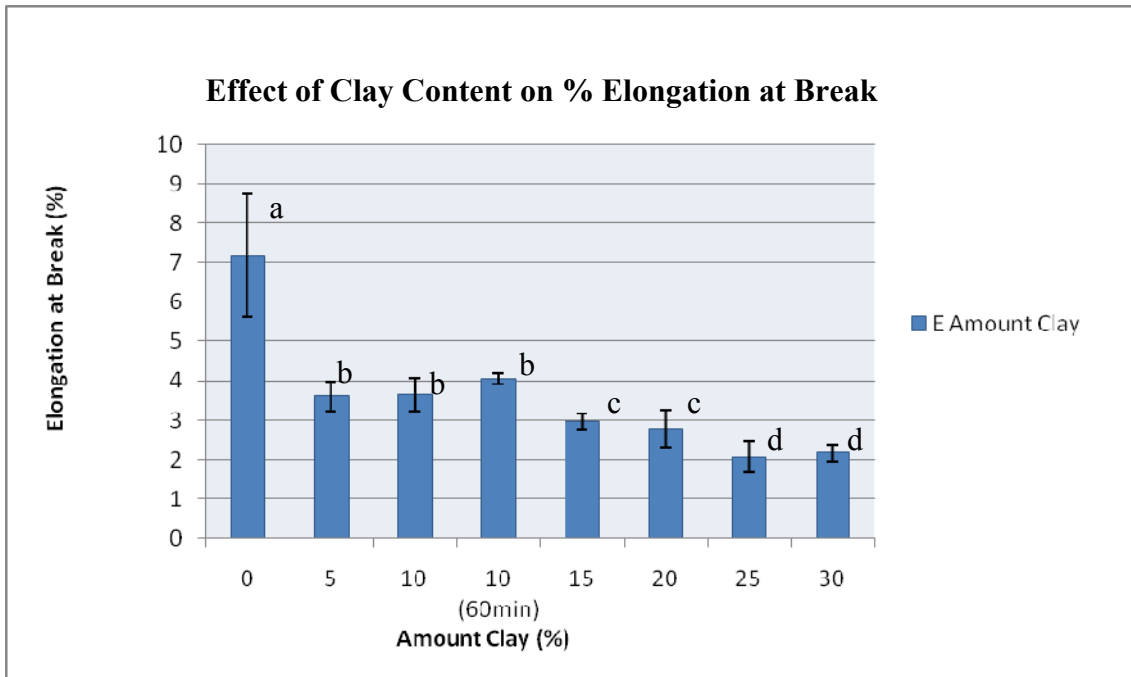


**Figure 23: Elongation at Break (%), Batch Clay Amount**

Figure 23 illustrates how all specimen incurred lower EB values with the addition of Cloistie Na+. The 5 and 10% clay samples are statistically indifferent and have lower EB values compared to the control. The 15% and 20% clay samples show low EB (less than 3%). Increasing the clay content of the films lowers the EB; this is revealed by the 25 and 30% composite films. Both Figure 22 and Figure 23 illustrate that the addition of clay reduces EB. Increasing ultrasonification times do not influence the EB. When EB decreases and the TS increases the clay particles have reinforced the matrix (increasing



tensile) but have weakened the starch matrix (decreases EB). Similar research examined how immiscible additives (i.e. clay) reduce the EB properties. Results indicated that when an additive was dispersed into a "ductile matrix," portions of the matrix material became fragile (St-Pierre et al, 1997). A similar behavior has been reported by Mondragon (2008). This explains why the weakening of the matrix only effects the EB properties. The addition of nanoclay strengthens the film matrix, yet prevents it from achieving an EB value equal to a pure starch matrix.

### Oxygen Permeability

**Table 15: Oxygen Permeability, batch ultrasonification time**

| <b>Ultrasonification Time (min)</b>   | <b>Clay amount (wt%)</b> | <b>O<sub>2</sub>Permeability (cc-mil/(m<sup>2</sup>-day))<sup>x</sup></b> |
|---|--------------------------|---|
| 0   | 0                        | 9.00 ± 2.60 <sup>a*</sup>   |
| 0   | 5                        | 5.40 ± 2.49 <sup>ab*</sup>  |
| 5   | 5                        | 5.28 ± 2.36 <sup>ab*</sup>  |
| 10  | 5                        | 5.71 ± 2.34 <sup>ab*</sup>  |
| 30  | 5                        | 4.71 ± 1.73 <sup>ab*</sup>  |
| 60  | 5                        | 2.36 ± 0.27 <sup>b*</sup>   |
| <sup>x</sup> Permeability is measured at 23 degrees Celsius and 50% RH<br><sup>*</sup> Means with the same letter are not significantly different |                          |   |

Table 15 shows how oxygen permeability decreased with the addition of ultrasonified clay. All samples had a uniform thickness of  $84.46 \pm 13.32$  micrometer. The quality of

oxygen barrier is directly associated with the dispersion of nanoclay. Ultrasonification time of 30 minutes did significantly effect OP when compared to non ultrasonification. Increasing the ultrasonification time above 30 minutes did not significantly effect oxygen permeability, as seen for both samples containing 10% clay. Thus, oxygen permeability is a function of ultrasonification time. When clay sheets are exfoliated, layers are delaminated from the clay creating a “torturous path” for oxygen to move through. Increased clay dispersion creates a challenging path for oxygen to permeate through the starch composite matrix (Figure 4).

**Table 16: Oxygen Permeability, batch amount clay**

| <b>Cloisite Na+<br/>(wt%)</b>  | <b>Ultrasonification<br/>Time (min)</b> | <b>O<sub>2</sub> Permeability (cc-mil/(m<sup>2</sup>-day))<sup>a</sup></b> |
|--|---|--|
| 0  | 0                                       | 12.63 ± 3.09 <sup>a*</sup>   |
| 5  | 30                                      | 5.84 ± 1.10 <sup>b*</sup>  |
| 10   | 30                                      | 5.43 ± 1.30 <sup>b*</sup>  |
| 10   | 60                                      | 5.99 ± 2.26 <sup>b*</sup>  |
| 15   | 30                                      | 4.74 ± 1.17 <sup>b*</sup>  |
| 20   | 30                                      | 4.47 ± 1.35 <sup>b*</sup>  |
| 25   | 30                                      | 4.94 ± 0.99 <sup>b*</sup>  |
| 30   | 30                                      | 4.11 ± 0.78 <sup>b*</sup>  |
| <sup>a</sup> Permeability is measured at 23 degrees Celsius and 50% RH |   |  |
| * Means with the same letter are not significantly different           |   |  |

Table 16 shows how oxygen permeability is affected by the addition of clay. Interestingly, the percentage of clay in the film does not significantly differ from 5-30% wt clay content. However, the data shows a slight, but not statistically significant, trend that as clay content increases, OP decreases. The lowest OP results were obtained for samples with 30% wt clay content.

In general, increasing crystallinity of a polymer reduces oxygen permeability. The addition of a clay has a similar effect. The clay layers improve the oxygen barrier of the film due to forming a tortuous path. The permeability rates were statistically insignificant with the further addition of clay. This phenomenon can be explained by the degree of dispersion of the clay platelets. As the clay content in the film increases, it becomes more difficult to reach full exfoliation. Theoretically, the greater the exfoliated clay content, the greater the oxygen barrier. However, it becomes increasingly difficult to fully exfoliate high clay contents (>15%), and therefore a more optimal “tortuous path” could not be achieved by the addition of more clay.

### **Water Vapor Permeability**

Table 17 shows the effect of ultrasonification time on water vapor permeability (WVP). WVP was calculated using ASTM cup method (ASTM E96). Film thickness was  $88.81 \pm 8.40$  micrometer for all samples.

**Table 17: Water Vapor Permeability, batch ultrasonification time**

| <b>Ultrasonification time (min)</b>                          | <b>Clay (wt %)</b> | <b>WVP (ng m/m<sup>2</sup> s Pa)</b> |
|--|--------------------|--------------------------------------|
| 0  | 0                  | 0.51980 ± 0.0551 <sup>a*</sup>       |
| 0  | 5                  | 0.52690 ± 0.0712 <sup>a*</sup>       |
| 5  | 5                  | 0.42020 ± 0.0742 <sup>b*</sup>       |
| 10   | 5                  | 0.4998 ± 0.0295 <sup>ab*</sup>       |
| 30   | 5                  | 0.49070 ± 0.0196 <sup>ab*</sup>      |
| 60   | 5                  | 0.47830 ± 0.0030 <sup>ab*</sup>      |
| * Means with the same letter are not significantly different |                    |                                      |

An analysis of the WVP of starch and composite films yielded that ultrasonified composite specimens have lower permeability rates than non-composite films. Lower permeability rates indicate increased water barrier properties for composite films. This can be attributed to the excellent barrier properties of Cloisite Na<sup>+</sup> clay. It should be noted that film samples treated with ultrasonification showed decreased WVP when compared to the control sample and the non ultrasonified samples. However, longer ultrasonification times did not improve WVP. The dispersed clay displaces free water and reduces the free volume in the film matrix, resulting in better WVP compared to films with no clay addition.

**Table 18: Water Vapor Permeability: Batch Amount Clay**

| Clay (wt %)  | Ultrasonification |                                |
|--|-------------------|--------------------------------|
|  | Time (min)        | WVP (ng m/m <sup>2</sup> s Pa) |
| 0  | 0                 | 0.57460± 0.0799 <sup>a*</sup>  |
| 5  | 30                | 0.49150± 0.0502 <sup>ab*</sup> |
| 10   | 30                | 0.5169 ± 0.0136 <sup>ab*</sup> |
| 10   | 60                | 0.5402 ± 0.0437 <sup>ab*</sup> |
| 15   | 30                | 0.5190 ± 0.0312 <sup>ab*</sup> |
| 20   | 30                | 0.5070 ± 0.0521 <sup>ab*</sup> |
| 25   | 30                | 0.4519 ± 0.0603 <sup>b*</sup>  |
| 30   | 30                | 0.4405 ± 0.0826 <sup>b*</sup>  |
| * Means with the same letter are not significantly different |                   |                                |

WVP properties were improved for films with clay (Table 18). Specimens with 5 to 20% clay were significantly different than samples with 25 and 30% clay. The greater the clay content, the lower the WVP. The samples with less than or equal to 20% wt clay were not significantly different. Interestingly, samples with 5% and 10% clay content had the greatest clay dispersion, but not the lowest WVP. Therefore, it could be argued that the 5% and 10% wt samples enhance barrier properties due to greater clay exfoliation, which is not seen in higher clay samples. Due to excellent clay dispersion, the engagement of OH groups within the layers makes the film less attracted to water absorption. Thus, it is possible to hypothesize that greater barrier properties can be achieved for higher clay

content samples if dispersion can be improved by other factors such as longer ultrasonification times. However, the 10% clay samples ultrasonified for 60 minutes showed no difference when compared to 10% clay samples ultrasonified for 30 minutes because both film specimens were completely exfoliated.

## Color and Haze

**Table 19: Color measurements: Batch ultrasonification time**

| <b>Ultrasonification Time (min)</b>                          | <b>L</b> | <b>a</b> | <b>b</b> | <b>Haze (%)</b>            | <b>Δ E</b>                 |
|--|----------|----------|----------|----------------------------|----------------------------|
| Starch   | 98.52    | 0.65     | 0.49     | 62.32 ±0.037 <sup>b*</sup> | 0.053± 0.03 <sup>e*</sup>  |
| 0  | 95.88    | 0.25     | 2.40     | 66.90 ±2.55 <sup>a*</sup>  | 3.280± 0.35 <sup>a*</sup>  |
| 5  | 98.11    | 0.20     | 1.78     | 60.10 ±0.63 <sup>b*</sup>  | 1.430± 0.05 <sup>d*</sup>  |
| 10   | 98.13    | 0.14     | 2.00     | 62.48 ±1.09 <sup>b*</sup>  | 1.650± 0.11 <sup>cd*</sup> |
| 30   | 98.30    | -0.04    | 2.48     | 62.69 ±2.01 <sup>b*</sup>  | 2.130± 0.08 <sup>b*</sup>  |
| 60   | 97.88    | 0.12     | 1.92     | 62.33 ±1.32 <sup>b*</sup>  | 1.770± 0.13 <sup>c*</sup>  |
| * Means with the same letter are not significantly different |          |          |          |                            |                            |

Table 19 shows all color values and haze for the samples tested. Color difference ( $\Delta E$ ) varied between 1.43 and 3.28. All samples tested were significantly different when compared to the control (yellowish color). The greatest color difference was observed for samples which were not ultrasonified. This could be due to the improperly dispersed clay in the film matrix. The haze values were not significantly different for samples with different ultrasonification times. Only S0C5 showed a significant difference in haze, most likely because it was not ultrasonified and had a poor dispersion of clay in the matrix. All film samples had a color change towards yellow due to the fact that Cloisite Na<sup>+</sup> is yellowish in color. However, there was no optical difference detected by the researcher's eye between the clay samples.








**Table 20: Color measurements, Batch amount clay**

| <b>Clay (wt %)</b> | <b>L</b> | <b>a</b> | <b>b</b> | <b>Haze (%)</b>             | <b>Δ E</b>                |
|--------------------|----------|----------|----------|-----------------------------|---------------------------|
| 0                  | 98.30    | 0.35     | 0.51     | 57.60 ± 1.28 <sup>c*</sup>  | 0.00 ± 0.03 <sup>e*</sup> |
| 5                  | 97.67    | 0.12     | 1.38     | 62.10 ± 1.70 <sup>b*</sup>  | 1.10 ± 0.19 <sup>d*</sup> |
| 10                 | 96.89    | -0.24    | 2.92     | 62.19 ± 2.88 <sup>b*</sup>  | 2.87 ± 0.44 <sup>c*</sup> |
| 10 (60minSon.)     | 97.49    | -0.59    | 3.84     | 62.84 ± 1.29 <sup>b*</sup>  | 3.26 ± 0.06 <sup>c*</sup> |
| 15                 | 96.38    | -0.23    | 3.21     | 61.81 ± 2.19 <sup>b*</sup>  | 3.02 ± 0.47 <sup>c*</sup> |
| 20                 | 95.73    | -0.23    | 3.81     | 65.86 ± 0.93 <sup>ab*</sup> | 4.22 ± 0.36 <sup>b*</sup> |
| 25                 | 95.30    | -0.20    | 3.61     | 63.14 ± 1.50 <sup>b*</sup>  | 3.36 ± 0.10 <sup>c*</sup> |
| 30                 | 94.15    | -0.28    | 5.01     | 69.70 ± 1.29 <sup>a*</sup>  | 6.17 ± 0.06 <sup>a*</sup> |



Table 20 shows how color difference ( $\Delta E$ ) was affected by the addition of nanoclay. The clay sample with 5% and 10% wt showed the lowest color differences, whereas the addition of more clay resulted in a noticeable color difference (towards b-value). Table 21 illustrates how the addition of clay caused the film to become more yellow. The Haze value increased also with the addition of nanoclay. Higher clay samples are more opaque than lower clay films and the control.

**Table 21: Appearance composite films**

| Clay 0<br>(wt %)   | Clay 5<br>(wt%)  | Clay 10<br>(wt %)  | Clay 15<br>(wt %)  | Clay 20<br>(wt %)   | Clay 25<br>(wt %)  | Clay 30<br>(wt %)  |
|--|--|--|--|---|--|--|
|  |  |  |  |  |  |  |

## CHAPTER FIVE

### V. CONCLUSIONS

Mung bean starch and nanoclay showed an expected affinity to each other since both have a hydrophilic structure. A starch clay composite film was easily produced in conjunction with water and glycerol. The dispersion of clay in the film matrix was controlled by ultrasonification, allowing intercalation and exfoliation of the clay layers. TS was increased to a maximum of 58% compared to non-composite mung bean starch. Barrier properties were improved significantly. The oxygen permeability was reduced from  $12.63 \pm 3.09$  cc-mil/m<sup>2</sup>/day for a pure mung bean starch film to  $4.11 \pm 0.78$  cc-mil/m<sup>2</sup>/day for a 30% wt clay film ultrasonified for 30 minutes. WVP improved from  $0.5746 \pm 0.0799$  ng m/m<sup>2</sup> s Pa for the control film to  $0.4405 \pm 0.0826$  ng m/m<sup>2</sup> s Pa for a film with 30% wt clay ultrasonified for 30 minutes. The greatest barrier improvements were obtained from films containing the greatest amount of Cloisite Na<sup>+</sup>. Film with desirable properties and appearance was achieved with less clay addition. The addition of clay greater than 10% affected the appearance of the film such (i.e. increasing the Haze and  $\Delta E$ ). The X-Ray Diffraction Pattern as well as the TEM images illustrated the degree of clay dispersion. Results indicated how proper ultrasonification time and the specific addition of nanoclay enhances the mechanical and barrier properties of mung bean composite films. These results can be attributed to proper clay dispersion. Only 5% wt Cloisite Na<sup>+</sup> samples had improved TS and oxygen permeability properties while maintaining maximum optical appearance. However, adding more clay to the matrix did

not result in an increase of mechanical strength. High clay sample films (20 to 30%) showed lower mechanical strength when compared to the control, which can be related to the poor exfoliation of clay (clearly illustrated in the X-Ray Pattern and TEM images). The addition of clay had an effect on the WVP, because Cloisite Na<sup>+</sup> drastically decreases amorphous regions in the mung bean starch, however ultrasonification time had no effect beyond a base time of 5 minutes. EB increased significantly for all clay composites, independent of ultrasonification time. Overall, the addition of low clay illustrated the greatest mechanical strength and improved the barrier properties. The optimum clay amount was found to be 5% wt Cloisite Na<sup>+</sup> and ultrasonified for 30 minutes.

## CHAPTER SIX

### VI. FUTURE RESEARCH

Theoretically, a mung bean starch/nanoclay composite film could act as a layer in a multilayer film. These films would be reasonable substitutes for conventional polymer films and could be implemented into various packaging applications. Water vapor properties could be improved by combining the composite film with a non polar polymer. Further research could develop a method of creating biodegradable multilayer film, having excellent mechanical, barrier and appearance properties.

Future research could entail a further investigation of the dispersion of clay in the starch matrix by focusing on other factors influencing the dispersion of high clay amount composites. Research could also investigate a method to create oriented clay particles in starch composite films to compare mechanical and barrier properties to non oriented composite films. Theoretically, oriented clay particles, if optimally distributed in the matrix, could further improve properties because the matrix would show an excellent ordered path.

Also, different packaging relevant properties, such as sealing strength properties of starch-clay composite films could be studied. Sealing of thermoplastic materials is an important film property when forming a package. Research could concentrate on identifying the critical parameters and sealing methods for starch-clay films.

Another interesting research investigation could be a concrete comparison of the complete life circle of starch based composite polymers and conventional plastics. The life cycle assessment includes all environmental inputs and outputs, real emissions and waste over the products life cycle. The research could show if and how a biodegradable starch composite film affects the environment compared to an oil based film with similar properties.

## REFERENCES

- ASTM, (1993). "Standard Test Method for Water vapor Transmission of Materials.", Standard Designation E96-93. Annual Book of ASTM, ASTM, 771- 778., Philadelphia, USA.
- ASTM, (2001). "Standard Terminology Relating to Plastics.", Standard Designation D 883-00., Annual Book of ASTM Standards, ASTM, 169-178., Philadelphia, USA.
- ASTM, (2002). "Standard Test Method for Oxygen Gas Transmission Rate Through Plastic Film and Sheeting Using a Coulometric Sensor.", Standard Designation D 3985-02., Annual Book of ASTM Standards, ASTM, Philadelphia, USA.
- Bae, H. J. Cha, D. S. Whiteside S. W. and H. J. Park, (2007). "Film and Pharmaceutical Hard Capsule Formation Properties of Mungbean, Waterchestnut, and Sweet Potato Starches.", Food Chemistry 106, 96-105.
- Bellis, M. (1997). "Cellophane.",  
<http://inventors.about.com/library/inventors/blcellophane.htm>, as of 18.11.08.
- Bertuzzi, M.A., Vidaurre, C., Armada, M. and J.C. Gottifredi, (2006). "Water vapor permeability of edible starch based films.", Journal of Food Engineering 80, 972-978.
- Brandon, D. and W. Kaplan, (1999). "Microstructural Characterization of Materials.", England, UK.
- Brown, G., (1961). "The X-Ray Identification and Crystal Structures of Clay Minerals.", Mineralogical Society, London, England.
- Brown, S., (1991). "Vegetarian Cookery.", Pocket Encyclopedia., Dorling Kindersley, London, England.

- Chaudhary, D.S., (2008). "Understanding Amylose Crystallinity in Starch-Clay Nanocomposites.", *Journal of Polymer Science: Part B: Polymer Physics*, Vol. 46, 979-987.
- Clarke, G., (1989). "Industrial Clay, a special review.", Industrial Minerals, New York, USA.
- Cyras, V. P. Manfredi, L. B. Ton- That, M.-T. and A. Vazquez, (2007). "Physical and Mechanical Properties of Thermoplastic Starch/ Montmorillonite Nanocomposite Films.", *Carbohydrate Polymers* 73, 55-63.
- Darder, M. Aranda, P. and E. Ruiz-Hitzky, (2007). "Bionanocomposites: A new Concept of Ecological, Bioinspired, and Functional Hybrid Materials.", *Advanced Material* vol. 19, no. 10, 1309-1319 .
- Dean, K., Yu, L. and D.Y. Wu, (2006). "Preparation and Characterization of Melt-extruded Thermoplastic Starch/Clay Nanocomposites.", *Composites Science and Technology* 67, 413 -421.
- Epic, Environmental and Plastics Industry Council, (2000). "Biodegradable polymers: A Review", Technical Report.
- Habig, T. McHugh, Avena-Bustillos R. and J.M. Krochta, (1993). "Hydrophilic Edible Films: Modified Procedure for Water Vapor Permeability and Explanation of Thickness Effects.", *Journal of Food Science* vol. 58, no.4, 899-903.
- Hamerton, I. (2003). "Polymers, the Environment and Sustainable Development", University of Surrey, Guildford, UK.
- Henrique, C. M. Teofilo, R.F. Sabino L. Ferreira, M. M. C. and P. Ceredam, (2007). "Classification of Cassava Starch Films by Physicochemical Properties and Water Vapor Permeability Quantification by FTIR and PLS." *Journal of Food Science*, vol. 72, no.4, 184-189.

Hunter Lab, The Color Management Company, Universal Software Version 3.2 and Above Users Manual, Manual Version 1.5 (Glossary, 20-3)

IT IS Report (2008). "Vigna Radiata (L.) R. Wilczek", <http://www.itis.gov>, as of 11.18.08.

Krishnamoorti, R. and R. A. Vaia, (2002). "Polymer Nanocomposites, Synthesis, Characterization, and Modeling (ACS Symposium Series 804).", USA.

Lawton, J.W., (1996). "Effect of Starch Type on the Properties of Starch Containing Films.", Carbohydrates Polymer 29, 203-208.

Mallapragada, S. and B. Narasimhan, (2006). "Biodegradable Polymeric Materials and Their Applications.", CA, USA.

McMurry, J. and R.C. Fay , (2001). "Chemistry.", 3<sup>rd</sup> ed., New Jersey, USA

McHugh, H.T., Avena-Bustillos, R. and J.M. Krochta, (1993). "Hydrophilic Edible Films: Modified Procedure for Water Vapor Permeability and Explanation of Thickness Effects.", Journal of Food Science, vol. 58, no.4, 899-903.

Means, R.E. and J.V. Parcher, (1963). "Physical Properties of Soils.", Oklahoma State University, Ohio, USA.

Mehyar, G.F. and J.H. Han, (2004). "Physical and Mechanical Properties of High Amylase Rice and Pea Starch Films as Affected by Relative Humidity and Plasticizer.", Journal of Food Science, vol. 69, Nr. 9, 449-454.

Mermut, A.R., (1994)., "Layer Charge of 2:1 Silicate Clay Minerals.", The Clay Mineral Society, Volume 6, SK, Canada.

Mondragon, M. Mancilla J. E. and F. J. Rodriguez-Gonzalez, (2008). "Nanocomposites from Plasticized High-Amylopectin, Normal and High-Amylose Maize Starches.", Polymer Engineering and Science, 1261-1267.



- Motavalli, J., (2001). "Zero Waste", The Environmental Magazine, vol. 12,  
<http://www.emagazine.com/view/?506>, as of 08.12.2008.
- Osswald, T.A. and G. Menges , (1995). "Material Science of Polymers for Engineers.",  
New York, USA.
- Pandey, J. K. and R. P. Singh, (2005). "Green Nanocomposites from Renewable  
Resources: Effect of Plasticizer on the Structure and Material Properties of Clay-  
filled Starch.", Starch 57, 8-15.
- Park, H.-M. Li, X. Jin, C.-Z. Park, C.-Y. Cho, W.-J. and C.-S. Ha, (2002). "Preparation  
and Properties of Biodegradable Thermoplastic Starch/Clay Hybrids.",  
Macromolecular Materials and Engineering, 287 no.8, 553-558.
- Rule, A.C. and S. Guggenheim, (2002). "Teaching Clay Science, Workshop lecture.",  
The Clay Minerals Society, Volume 11, Auora, CO
- Selke, S.E.M. Culter, D.J. and R.J. Hernandez, (2004). "Plastic Packaging, Properties,  
Processing, Applications, and Regulations.", 2<sup>nd</sup> ed., Cincinnati, USA.
- Subramanian, P.M. (2000). "Plastics recycling and waste management in the US."  
Resources, Conservation, and Recycling 28, 253-263.
- Smith, R. (2000). " Biodegradable Polymers for Insustrial Applicatons.", Florida, USA.
- Soroka, W., (1999). "Fundamentals of Packaging Technology.", 2<sup>nd</sup> ed., VA, USA.
- Steinbuechel A., (2003). "Biopolymers, General Aspects and Special Applications.", vol.  
10, Muenster, Germany.
- Stevens, E. S. (2002). "Green Plastics, An Introduction to the New Science of  
Biodegradable Plastics.", Princeton, New Jersey, USA. (52)

- St-Pierre, N. FAVIS, B. D. Ramsay, B. A. Ramsay, J. A. and H. Verhoogt, (1997).  
“Processing and Characterization of Thermoplastic Starch/Polyethylene Blends.”,  
Polymer, vol. 38, no.3, pp. 647-655.
- The Sustainable Packaging Coalition, (2005). “Definition of Sustainable Packaging.”,  
<http://www.sustainablepackaging.org/pdf/Definition>, as of 11.18.08.
- Theng, B.K.G., (1979). “Formation and Properties of Clay-Polymer Complexes.  
Developments in soil science 9.”, New York, USA.
- Whistler, R. L. and J. BeMiller, (1997).”Carbohydrate Chemistry for Food Scientists.”,  
Minnesota, USA.
- Whistler, R. L., BeMiller, J. N. and E. F. Paschall, (1984). “Starch, Chemistry and  
Technology.”, 2<sup>nd</sup> ed., Florida, USA.
- Wikipedia, the free Encyclopedia, <http://en.wikipedia.org/wiki/Montmorillonite>, as from  
09.16.2008.
- Wischnitzer, S., (1962). “Introduction to Electron Microscopy.”, New York, USA.